ARL-CR-0837 ● DEC 2018

US Army Research Laboratory

Opportunities and Application of Morphing Airframe Technology for Projectiles

prepared by Bryant Nelson
Bennett Aerospace
459 Mulberry Point Road, Room 300M
Aberdeen Proving Ground, MD 21005

under contract W911QX-D-0014

NOTICES

Disclaimers

The findings in this report are not to be construed as an official Department of the Army position unless so designated by other authorized documents.

Citation of manufacturer's or trade names does not constitute an official endorsement or approval of the use thereof.

Destroy this report when it is no longer needed. Do not return it to the originator.

ARL-CR-0837 ● DEC 2018

US Army Research Laboratory

Opportunities and Application of Morphing Airframe Technology for Projectiles

prepared by Bryant Nelson
Bennett Aerospace
459 Mulberry Point Road, Room 300M
Aberdeen Proving Ground, MD 21005

under contract W911QX-16-D-0014

REPORT DOCUMENTATION PAGE

Form Approved
OMB No. 0704-0188

1. REPORT DATE *(DD-MM-YYYY)*	2. REPORT TYPE	3. DATES COVERED (From - To)
December 2018	Contractor Report	1 September 2015–31 May 2018

4. TITLE AND SUBTITLE
Opportunities and Application of Morphing Airframe Technology for Projectiles

5a. CONTRACT NUMBER
W911QX-D-0014

5b. GRANT NUMBER

5c. PROGRAM ELEMENT NUMBER

6. AUTHOR(S)
Bryant Nelson

5d. PROJECT NUMBER

5e. TASK NUMBER

5f. WORK UNIT NUMBER

7. PERFORMING ORGANIZATION NAME(S) AND ADDRESS(ES)
Bennett Aerospace
459 Mulberry Point Road, Room 300M
Aberdeen Proving Ground, MD 21005

8. PERFORMING ORGANIZATION REPORT NUMBER
ARL-CR-0837

9. SPONSORING/MONITORING AGENCY NAME(S) AND ADDRESS(ES)
US Army Research Laboratory
ATTN: RDRL-WML-F
Aberdeen Proving Ground, MD 21005-5069

10. SPONSOR/MONITOR'S ACRONYM(S)
ARL

11. SPONSOR/MONITOR'S REPORT NUMBER(S)

12. DISTRIBUTION/AVAILABILITY STATEMENT
Approved for public release; distribution is unlimited.

13. SUPPLEMENTARY NOTES

14. ABSTRACT
The bulk of morphing airframe technology research over the past several decades has been geared toward commercial and military aircraft and rotorcraft platforms, but implementation has proven difficult due to complicating factors such as scalability, repeatability, reliability, weight, and cost. This review report looks at these and other emerging technologies with respect to projectiles, where many of these factors are relaxed. Projectiles are distinct from other types of munitions such as missiles, rockets, and bombs due to their cylindrical initial body conditions, lack of onboard propulsion and therefore cruise velocity, relatively small size, relatively low cost, and the extreme shock event at gun launch. Despite these challenges, projectiles are single-use systems with short flight durations, which decreases the reliability and repeatability constraints that have limited the implementation of morphing concepts on full-scale aircraft. These characteristics make projectiles an ideal platform for emerging morphing concepts, especially when factoring in the desire for range extension, maneuverability, and mission flexibility. This report reviews previously implemented and emerging morphing strategies, including smart materials, morphology-dependent structures, and fluid-driven actuators such as shape memory alloys, piezoelectric actuators, macro-fiber composites, active polymers, compliant structures, periodic cellular structures, bistable composites, inflatable structures, pressurized artificial muscles, and soft actuators.

15. SUBJECT TERMS
morphing, shape memory alloy, piezoelectric, macro-fiber composites, active polymers, compliant mechanisms, bistable structures, inflatable structures, pressurized artificial muscles, soft robotics

16. SECURITY CLASSIFICATION OF:			17. LIMITATION OF ABSTRACT	18. NUMBER OF PAGES	19a. NAME OF RESPONSIBLE PERSON
a. REPORT	b. ABSTRACT	c. THIS PAGE			Bryant Nelson
Unclassified	Unclassified	Unclassified	UU	66	19b. TELEPHONE NUMBER (Include area code) 410-306-1211

Contents

List of Figures

1. Introduction

The goal of this report is to present a broad overview of morphing airframe technologies and investigate how they have or could be incorporated into precision guided projectiles. Morphing is defined in this report as a controlled shape change of an existing continuous structure. While an argument could be made that simple deployable control surfaces such as those investigated in Fresconi et al.[1] could fit this definition, such simplistic, well-understood systems have been excluded from this analysis because the control surface itself is not morphing; rather, it is merely being deployed from a stowed state. This report considers morphing technologies for active projectile control as well as gradual deformations that enhance flight performance.

Projectiles present several challenges for designers. First, projectiles are typically gun-launched systems; therefore, all hardware must survive the extreme in-bore environment to accomplish the objective. Launch accelerations typically range from 7000 to 100,000 g's (Fig. 1). Second, projectiles must conform to cylindrical initial body conditions imposed by the barrel, which pose significant packaging challenges and drastically limit the size of traditional wings and control surfaces. Third, projectiles are much, much smaller than commercial aircraft where the bulk of morphing technology research is geared. Fourth, projectiles, unlike missiles, typically do not have any means of onboard propulsion. All energy available for maneuvering is stored and released at gun launch. This places significant emphasis on the control actuation system to utilize that energy in the most efficient manner. Some projectiles incorporate an onboard rocket motor; however, this motor is usually ignited by the gun gases and burns out prior to the deployment of any control surfaces at apogee. Much of the material presented can be applied to other munition systems such as rockets, missiles, and bombs; however, not all the constraints listed necessarily apply.

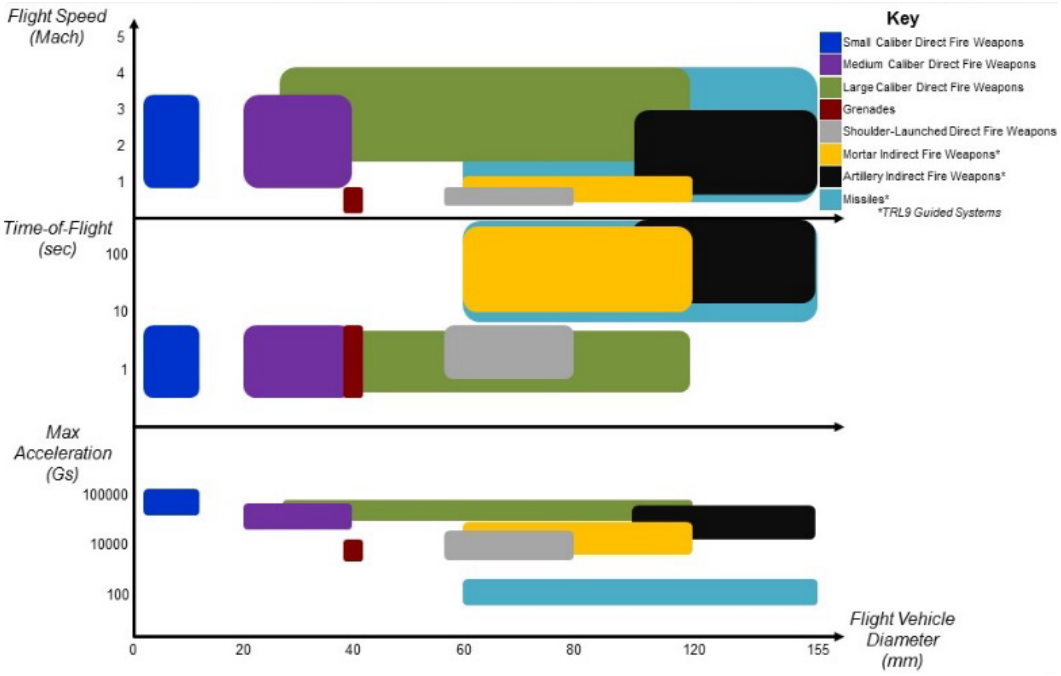

Fig. 1 Velocity, time of flight, and peak acceleration for several classes of projectiles compared with missiles

Projectiles also present several advantages to the designer, the first of which is that projectiles are single-use systems, which drastically reduces the reliability and repeatability constraints that apply to commercial aircraft. Projectiles also have a much shorter flight time than most air vehicles, typically on the order of seconds to minutes (Fig. 1). Therefore, actuators with limited cycle life or hysteresis that have been invalidated for use in commercial aircraft, which are expected to last decades (a 6–8 order of magnitude difference), can be incorporated into projectiles.

The morphing technologies presented can offer several advantages to projectiles, including maneuverability, range extension, omnisonic performance, and stealth. Maneuverability has already been identified as a crucial research area for projectiles to engage moving targets and avoid counter rocket, artillery, and mortar (CRAM) systems. Several of the morphing airframe technologies discussed herein could significantly reduce the radar cross section by using RF-transparent materials, which can help future projectiles avoid CRAM interceptors in contested airspace as well as enhance the effectiveness of friendly CRAM interceptors by not triggering a maneuvering response from an evasive target. Projectiles are also unique because they do not have a fixed cruise velocity and can transition several Mach regimes. An example, shown in Fig. 2, shows a single 155-mm projectile launched at five different charges zones, wherein Zone 1 remains entirely subsonic while Zone 5 goes from supersonic to transonic to subsonic, then back to the

transonic Mach regime. Morphing concepts are thus more applicable to omnisonic projectiles than other munitions that operate within a single Mach regime.

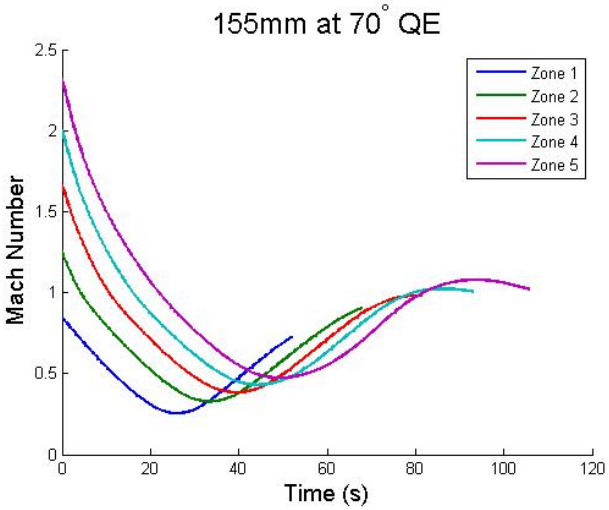

Fig. 2 Mach vs. time for 155-mm artillery at five charge zones using modular artillery charge system

All possible morphing modes have been investigated. These include translational morphing modes such as spanwise morphing, chordwise morphing, and airfoil profile morphing as well as rotational modes like wing sweep, an/dihedral morphing, and camber morphing. Wing twist has also been investigated but is essentially differential camber morphing and is analyzed as such. Each morphing mode has its own deflection, force, and bandwidth requirements depending on how they are implemented.

An/dihedral morphing is the least applicable to projectiles of all potential morphing modes. While spanwise bending can be used to increase stability or to a small extent roll control, this can be accomplished better through other means. An/dihedral morphing is most applicable for active aeroelastic control or for conformal wing storage in the context of projectiles.

Camber morphing is the primary morphing mode for increasing maneuverability of projectiles. Since this is used for active control, the actuator bandwidth requirements are higher. Fresconi et al. identified 10 Hz as a suitable bandwidth for projectile guidance.[2]

Airfoil profile morphing is essential for optimizing omnisonic projectile performance undergoing trajectories similar to those in Fig. 2. Figure 3 shows a comparison of a supersonic double wedge airfoil, a transonic National Advisory Committee for Aeronautics (NACA) 0012, and a subsonic NACA 2414. The aft 50% chord is relatively similar for all profiles, while the first 50% chord has the

greatest variance particularly between supersonic and transonic profiles. Actuation schemes to achieve such changes require a relatively low deflection, as shown in Fig. 3, low bandwidth because these changes occur on the order of seconds to minutes (Fig. 2), and moderate load requirements to maintain airfoil shape subjected to supersonic pressures.

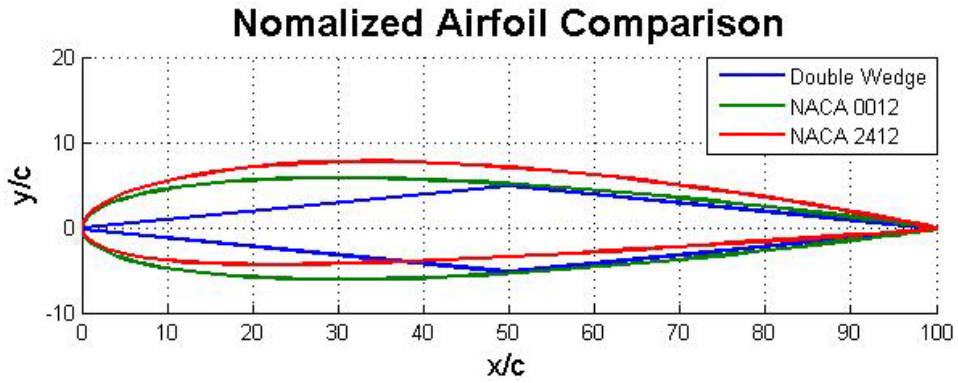

Fig. 3 Supersonic, transonic, and subsonic airfoil comparisons

Spanwise morphing is useful, as high-aspect-ratio wings have a higher lift-to-drag ratio $(L/D)^3$ but can also introduce unwanted aeroelastic phenomena. Since aeroelasticity and wing load are proportional to velocity, span can increase to a certain degree as the projectile decelerates without adverse effects. Spanwise morphing requires large deflections, low bandwidth, and low force.

Chordwise morphing can be useful for increasing wing area similarly to spanwise morphing, which in turn increases the forces generated. Chordwise morphing lowers the aspect ratio, which can increase the angle of attack (AoA) at stall, but also decreases L/D. The requirements for chordwise morphing are similar to spanwise morphing but with lower deflection requirements.

Changes in sweep are especially useful for omnisonic projectiles, as swept-back wings are more efficient supersonically. The required angle change is typically around 90° from the stowed state, and any actuator must be strong enough to overcome the airfoil drag. The bandwidth requirement is low for omnisonic applications; however, differential wing sweep might be useful for active control. This would drastically increase the bandwidth and to a lesser extent force and deflection.

The morphing airframe technologies described herein have the potential to bring missile-like performance to projectiles as well as substantial improvements over their baseline ballistic counterparts. Technologies investigated in the following sections include smart materials such as shape memory alloy, piezoelectric actuators, macro-fiber composites (MFCs), active polymers, morphology-

dependent structures such as compliant structures, periodic cellular structures, bistable composites, and fluid-driven actuators such as inflatable structures, pressurized artificial muscles, and soft actuators as well as their hybrids.

2. Shape Memory Alloys

Shape memory alloys (SMAs) are a class of metallic materials that exhibit two stable crystalline forms and can alternate between them at specific temperatures and/or strains. The parent or austenite phase has a body-center cubic structure compared with the martensite phase, which has a face-centered cubic crystalline structure.[4] Martensite can exist in two distinct forms, twinned and detwinned. Stress applied above a specific threshold causes twinned martensite to deform in shear into detwinned martensite, which persists after unloading.[5] It can then return to its original geometry by adding heat even under inelastic deformations as high as 8% for some nickel–titanium alloys.[6] These alloys, first manufactured by the US Naval Ordinance Laboratory in 1962,[7] are the most common SMA materials used for actuation and have since been commercialized under the trade names Nitinol[8] and Flexinol[9] and are available in wires, sheets, strips, films, and tubes.

There are two distinct macroscopic effects associated with SMA materials: the shape memory effect and the pseudo-elastic effect. The pseudo-elastic effect describes the phenomenon where SMA materials transitions from the austenite phase to the detwinned martensite phase without going through the twinned martensite phase. Since this only occurs at temperatures higher than the austenite transition temperature, the material begins to revert to the austenite phase immediately upon the removal of stress.[4] This effect has limited application for morphing projectiles because the strain is not stable at these temperatures.

At lower temperatures, the shape memory effect becomes the dominant phenomenon and has two modes: one-way and two-way shape memory effects. These differ only by the number of stable configurations and manufacturing. The one-way effect is simply an SMA that returns to its original shape through heating, while the two-way effect has two stable configurations at different temperatures created through extensive training. The two-way effect is usually achieved with SMAs that exhibit lower mechanical properties resulting in lower-performing actuators.[4]

Researchers supporting the Defense Advanced Research Projects Agency's Smart Wing program investigated SMA torque tubes for twist actuation. A 4-inch-long 1.125-inch-diameter tube with a 0.060-inch wall thickness was able to achieve 5° of twist over the span and an impressive 3,200 inch-lb of torque and used the wing box as the bias spring to return the torque tube to its martensite state.[10] The high

thermal mass limited the bandwidth to less than 0.2 Hz.[11] Despite the success during the first phase of the program, SMAs were abandoned for another actuation method with higher deflection and bandwidth. SMAs torque tubes have also been investigated as part of a hybrid system wherein the fore sections of a flap are controlled by SMAs and the terminal section is controlled by an electric motor with higher bandwidth.[12] Others used an electromechanical clutch to control a set of SMA torsional actuators for camber morphing, resulting in large deflections of 40°.[13]

SMAs have been investigated for camber morphing using antagonistic pairs of SMA actuators[14–16] as well as an elastomer/SMA adaptive skin.[17] SMA wires were also investigated for the Smart Wing program, resulting in control surface deflections up to 7.5°.[18,19] Other concepts use SMA sheets with bonded heating elements to actuate interlocking vertebral rib sections, resulting in larger changes in camber and twist (Fig. 4).[20,21] Similar methods have used a bias spring instead of another SMA actuator.[22,23]

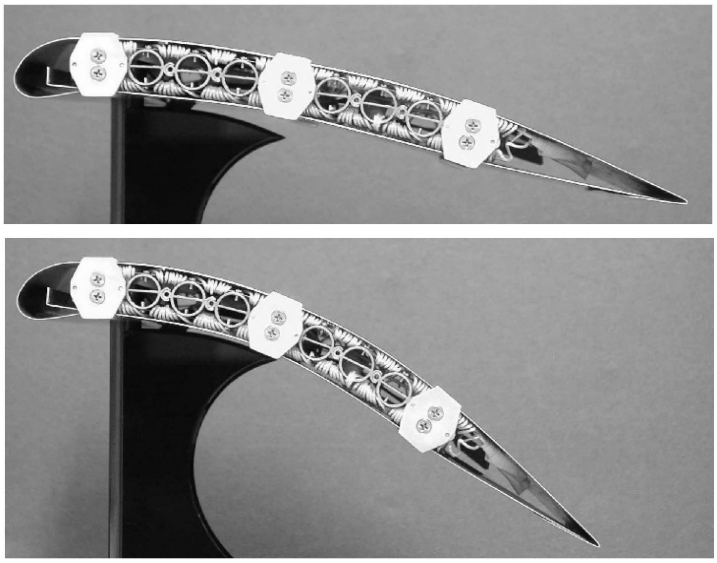

Fig. 4 Large camber change pre- and postactuation via an SMA actuator (Reprinted with permission from Elzey et al.[20])

SMAs have also been investigated for profile morphing to decrease boundary layer separation and wave drag by using a shock-reducing bump on the upper wing surface of transonic airfoils.[13,24,25] Wind tunnel experiments verified that a properly configured bump can reduce the overall wing drag by up to 22%.[24] Several researchers have used cam and crank mechanisms attached to the upper airfoil surface to amplify the deflection of SMAs.[26–29] Dong et al.[30] used SMA springs attached to the upper and lower skin surface to achieve airfoil profile morphing. These springs provide superior force and displacement compared with SMA wire due to the added length of the coiled structure.[30]

While SMAs have very high force-to-weight ratios,[31] they are limited by overall deflection and bandwidth. The deflection limitation has been addressed in two key ways: by sacrificing output force for mechanical amplification or by using longer wires. Since SMA deflection is a recovered, mechanically induced strain, the longer the material, the greater the deflection. Grant and Hayward took advantage of this by weaving multiple SMA wires into a helical pattern to increase deflection,[32] but this increased the thermal mass therefore decreasing bandwidth. A commercial off-the-shelf solution to the displacement problem exists in the form of Miga Motors, which are a series of SMA wires stacked to amplify their output.[33] By supplying the Miga Motors with approximately 2.5 times the recommended power, bandwidth increases from 1.3 to 2.5 Hz for up to 1.5 min before dropping back down.[34]

Bandwidth issues essentially invalidate noncooled SMAs for active projectile control in all but the most limited of cases due to the high bandwidth requirements. SMAs can still be used for morphing modes with lower bandwidth requirements such as spanwise, chordwise, or profile morphing. The bandwidth relies on the thermal mass and heat flux of the SMA actuator. SMAs can be actuated quickly through resistive heating[35,36] or though heating elements,[37] but take much longer to cool via natural convection.[38] Several methods have been employed to improve cooling, such as heat sinks,[39–41] forced-air convection,[42–44] super-cooled gas,[37] semiconductor heat pumps,[45] and liquid immersion.[46,47] In general, ambient air cooling can achieve bandwidths under 1 Hz, 4–6 Hz for forced air, and tens of hertz for liquid immersion in typical wire configurations. Wellman et al. demonstrated 40-Hz actuation frequencies using a recirculating coolant bath near the minimum austenite transition temperature.[47] Thin-film SMAs with low thermal mass have been used as fuel injectors with response times under 1 ms by using the working fluid for forced convective heat transfer.[48] Higher bandwidths can be achieved in micro-actuator applications with extremely low thermal mass without any active cooling. Research has demonstrated 30-Hz bandwidths at 2% strain for a 2.5-μm SMA film and 40-Hz bandwidth for smaller deflections.[40] Similar actuators have achieved up to 100-Hz actuation frequencies[49] all the way up to 2 kHz for submicron displacements.[38]

SMAs have potential for projectile shape morphing applications yet are limited by overall deflection and bandwidth. The bandwidth limitations constrain SMAs for active control to extremely small projectiles with lower deflection and force constraints. Actively cooling SMAs would be problematic from a weight, complexity, and shock survivability standpoint. Due to their lack of moving parts and robust nature, SMAs, in general, should survive shock as long as the martensite yield stress is not exceeded.

In hypersonic Mach regimes, high temperatures are generated by dissociation and ionization of air. This heat could be used to passively actuate SMAs incorporated into composites if properly insulated, but the transient response could introduce unwanted disturbances. Maximum achievable bending in SMA composites has been shown to be a function of SMA wire bond strength,[50] so SMA sheets may be a better choice. Such a control surface could deform continuously as the projectile decelerates and generates less heat, and should perform well in shock due to a lack of moving parts or electrical connections.

3. Piezoelectric Actuators

Piezoelectric actuators have been investigated for aircraft and munition morphing applications since the late 1980s due to their high force, high bandwidth, low weight, low part count, and ease of implementation and actuation.[51–53] Such actuators rely on the piezoelectric effect, which is a reversible, linear process where an applied electrical field generates mechanical strain. This differs from the electrostriction effect in that the material can both expand and contract due to the piezoelectric crystal anisotropy, which allows it to retain its polarization in the absence of an electric field.[54] The strain generated is an order of magnitude lower than SMAs, generally around 0.1%, but the bandwidth is several orders higher due to electrical instead of thermal activation. Since strain is based on crystal expansion, global strain is dependent on the overall length and output force is dependent on cross-sectional area. Piezo material can be manufactured in sheets, stacks, or directly incorporated into composites.

Piezo actuators have been used to create synthetic jets[55,56] and reciprocating tabs,[57] which alter the flow over flight bodies. While previous US Army Research Laboratory (ARL) efforts have demonstrated the effectiveness of this technique on projectiles,[58,59] such flow control techniques are outside the scope of this report, as they alter the flow without significant, if any, changes in the outer mold line.

Piezo actuators have successfully been incorporated into a variety of munitions. Recently, Dynamic Structures and Materials, LLC, incorporated their piezo stack actuators into a gun-launched projectile and successfully demonstrated survivability under gun-launch accelerations as well as hardware-in-the-loop integration. These actuators rely on a compliant external frame to amplify the strain generated by the piezo stack.[60] Others have demonstrated ±10° fin deflections up to 59 Hz during wind tunnel testing of a half-scale Mk 83 air-dropped munition using very long (31.8-inch) antagonistic lead zirconate titanate (PZT) plates.[61] A similar concept was applied to a gimbaled nose on a supersonic munition, which articulated the nose ±0.12° and survived launch loads up to 17,700 g's.

Precompression of the PZT material was shown to have a substantial, positive effect on gun-launch survivability.[62] This concept was later applied to the Barrel-Launched Adaptive Munition, where the actuator survived 9,300 g's with no deterioration in piezoceramic properties.[63] Barrett et al. expanded upon previous work[64–66] and created a twisting missile fin using directionally attached piezoelectric (DAP) actuators. These are piezo elements with a tailored bond area to reduce the transverse stiffness while maintaining longitudinal stiffness.[67] DAP actuators generated up to ±8.1° static pitch deflections with a corner frequency of 50 Hz.[68] Later improvements used orthogonally oriented PZT sheets, and subsonic wind tunnel experiments demonstrated tip deflections up to ±11°.[69,70]

Active fiber composites, wherein piezoceramic actuators are incorporated into the fiber layup of the aircraft's skin, have been investigated, but they tend to lack sufficient control authority.[71,72] Single crystal fiber composites such as those developed by Chiang et al.[73] have been suggested as potential improvements, but the actuation free strain is still below 1%, which limits its application especially when constrained within a fiber composite.

Piezoelectric elements have been investigated for active vibration damping and flap deflection on rotorcraft.[74–79] Two-stage amplification techniques have been used to amplify the stroke[74–75] as well as a multilayer piezo-bender concept.[76] The Boeing SMART active flap rotor demonstrated, for the first time, piezoelectric flaps on a full-scale MD 900 rotor in the wind tunnel at representative flight conditions (80 m/s) albeit with limited flap deflections of ±3°.[79]

In the 1990s, NASA patented several methods of manufacturing piezoelectric actuators with displacements several orders of magnitude greater than the pure piezoceramic.[80–83] Face International Corporation licensed and commercialized the actuators under the trademark THUNDER (THin Layer UNimorph Ferroelectric DrivER and Sensor).[84] These actuators are sandwiched piezoceramic wafers in between two electrically conductive substrates with differing thermal expansion coefficients (typically aluminum or stainless steel). The resulting product is a highly prestressed, curved piezoceramic composite that can achieve much higher deflections.[84]

Wind tunnel experiments investigated the potential of THUNDER actuators for airfoil profile morphing. The actuator was attached to the upper surface of the airfoil and covered with a flexible skin. While creep and hysteresis posed challenges, both appear to be bounded and eventually settled into stable displacement cycles.[85] Others investigated THUNDER actuators for camber morphing, but in wind tunnel testing the THUNDER actuators were consistently outperformed by traditional servo actuators.[86]

Another similar concept is Reduced And INternally Biased Oxide Wafer (RAINBOW) actuators, which also use thermal mismatch to prestress a piezoceramic. The difference is that RAINBOW actuators chemically reduce one side of a lead-containing piezoceramic to create a metallic layer within the actuator itself. Comparative studies have shown a 10%–25% increase in free displacement over THUNDER actuators.[87] Fatigue-induced displacement degradation of RAINBOW actuators under free displacement and loaded conditions has been investigated, showing a minimal decrease in displacement. For the unloaded cases, repoling the RAINBOW actuators restored the displacements to their initial values, while the loaded cases showed some degraded performance after repoling.[88]

Externally applied forces can also compress the piezo element to amplify its deflection and decrease its stiffness. The closer this load is to the column buckling load, the more electrical energy is converted to work.[89] Such actuators are referred to as postbuckled precompressed (PBP) actuators.[90,91] Unlike other techniques, the preload is not limited to thermal mismatch and can yield 2–6 times more stroke without compromising blocking force.[92–94]

Vos et al.[95] used PBP actuators for morphing wing tips, using the latex skin to apply the preload, which more than doubled the achievable deflection, resulting in a maximum deflection of 15.8°. Free-flight experiments demonstrated a 38% increase in roll authority, 3.7 times greater control derivatives, 3.5% decrease in weight, an order of magnitude increase in corner frequency and slop reduction, reduced part count, and 99% less power consumed than with conventional servo actuators.[95] PBPs have also been incorporated into a 25-mm chord control surface, shown in Fig. 5, resulting in unloaded pitch deflections of ±25° compared with ±2.6° using an uncompressed piezoceramic sheet. Wind tunnel experiments demonstrated pitch control up to ±22° at velocities up to 120 kt (62 m/s).[96] The scale, deflection, and bandwidth makes this design suitable for most medium- to large-caliber projectiles assuming it can operate at projectile velocities and survive gun launch.

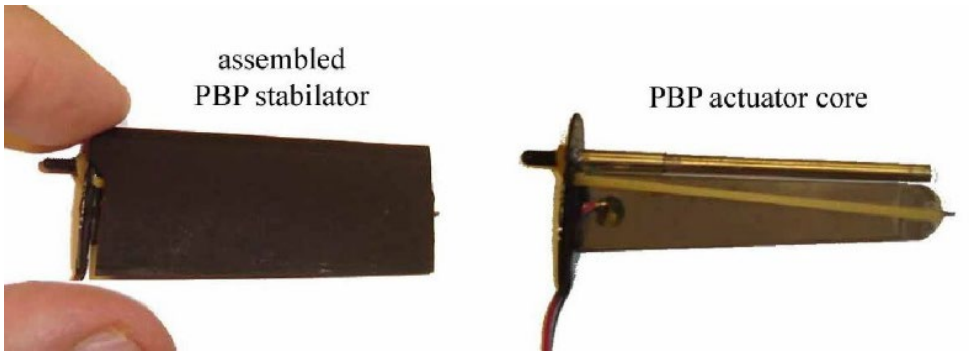

Fig. 5 Assembled control surface with and without aeroshell (Reprinted with permission from Barrett et al.[96])

The curvature of PBPs can introduce survivability issues due to tensile stress sensitivity of piezoceramics. To counteract this, researchers have incorporated hard stops into the actuator. One such technique incorporates a low-modulus convex silicone spacer attached to the PBP element and a high-stiffness face sheet attached to the end supports that carries some of the tensile load at high deflections[97,98] This concept, called dynamic elastic axis shifting, has been incorporated into a 6-inch transonic fin for a 250-lb-class weapon. Wind tunnel experiments demonstrated ±7° deflections up to 21 Hz at Mach 1.3 using 95% less power and substantially less space than conventional actuators.[99]

Bistable piezoelectric actuators have been investigated and can have larger displacements but cannot be controlled between stable configurations. A spring between the actuator and one of the boundaries can greatly reduce the voltage required for snap-through.[100] At low values the piezo actuator further compresses the spring without a transition, but at higher values the nonlinear dynamic snap-through behavior became more apparent.[101]

4. Macro-Fiber Composites (MFCs)

MFCs are a subclass of piezo actuators consisting of piezoceramic rods sandwiched between polyamide films embedded with interdigitated electrodes.[102] They were invented by NASA in 1996 and Smart Material Corporation has offered production-scale MFCs since 2002.[103] When voltage is applied, the composite expands, bents, twists, or vibrates depending on the rod orientation and input signal. If no voltage is applied, the MFC can function as a highly sensitive strain gauge or vibratory energy harvester.[103] MFCs have increased in popularity for morphing applications due to their flexibility, durability, high blocking force, low power, and ease of implementing the thin-film actuator into various concepts. MFCs are limited by their high voltage requirements, overall displacement, and hysteresis. The maximum operating frequency according to the datasheet is 10 kHz for actuator applications;[103] however, amplitude is limited and attaching the MFC to a substrate further limits displacement.[104]

MFCs have been investigated for camber morphing. Pankonien and Inman improved the overall deflection by 10.7% over a MFC hinged trailing edge by using a compliant “flexure box”.[105] Unimorph and bimorph configurations have been considered. The unimorph configuration uses one MFC for bending, whereas bimorph configurations apply MFCs to the top and bottom of a deflecting surface. While the bimorph configuration showed a 50% increase in stiffness, the unimorph configuration has a much larger actuation range.[106,107] The asymmetric voltage limits (–500 and +1500 V) were shown to account for this behavior.[106] Pankonien’s

variable camber wings showed a 34% increase in lift, 45% increase in rolling moment, 87% increase in pitching moment, as well as a 22% reduction in drag at off-design aerodynamic conditions.[108] A hybrid concept using SMA wire in conjunction with MFCs has been evaluated, resulting in a 45% increase in maximum lift over the MFC-only configuration and 180% increase over the SMA-only configuration (Fig. 6).[106,109]

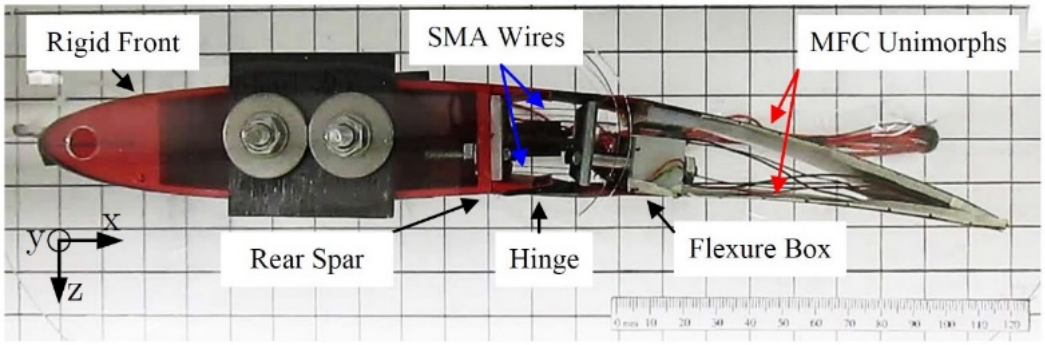

Fig. 6 Morphing aileron showing SMA and MFC smart material actuators (Reprinted with permission from Pakonien[106])

Flight experiments with a radio controlled airplane, in which all the control surfaces were replaced with bimorph MFC actuators, demonstrated the impact that severe lag and hysteresis had on the dynamic stability.[110] However, the airplane still flew, albeit not as well as the more maneuverable unmodified plane.[111] Others investigated the effects of various MFC support configurations on the trailing edge of a ducted fan vehicle.[112,113]

ILC Dover combined an inflatable wing with MFC actuators for trailing edge morphing and "bump flattening" of the inflatable spars. They found that the MFC actuators lacked the required force to overcome the inflation pressure needed to flatten the bumps. However, the bimorph MFCs mounted on the trailing edge achieved 3° of deflection.[114]

MFCs have also been used for airfoil profile morphing. Debiasi et al. mounted MFCs to the upper wing surface, which deformed the surface up to 2.1% of the chord.[115] Others investigated MFC-actuated bistable composite laminates for creating a drag-reducing bump on the upper wing surface. While the resultant stable shapes were predicted accurately, the MFC voltage required for snap-through proved challenging.[116] Schultz and Hyer improved on this by taking into account the local stiffening and curvature changes around the MFC actuator.[117]

ARL has investigated MFCs as alternative actuators, but preliminary feasibility studies in the wind tunnel resulted in time-dependent and hysteretic behavior as well as low levels of deflection.[118] Further research showed that a thinner core with

higher modulus was capable of achieving greater deflections without sacrificing torque or stiffness.[119] Despite these improvements, pure MFC-based morphing control surfaces for projectiles were abandoned due to their limited deflection. All MFC applications found in the literature have only been evaluated at low subsonic velocities, which are only applicable to the slowest projectiles (Fig. 1).

5. Active Polymers

This section covers shape memory polymers (SMPs) and dielectric elastomers (DEs). SMPs are polymers that can recover from a thermally conditioned strain though heating due to differences in Young's modulus above or below a phase transition temperature. For polyurethane-based SMPs, this occurs at the glass transition temperature (T_g) and at the crystalline melting temperature for trans-polyisoprene-based SMPs.[120] SMPs differ from SMAs in that they are lower in cost, lightweight, easier to program, and can recover substantially more strain. However, SMAs have much higher recovery stress, blocking force, and a higher thermal conductivity and therefore bandwidth. SMPs thermal conductivity can be improved by using SMP foams or incorporating conductive additives.[121] SMPs have a much higher Young's modulus below the phase transition temperature, which could limit SMP projectile applications since higher stiffness is desired at hotter, faster Mach numbers.

Cornerstone Research Group, Inc., commercialized Veriflex, an SMP capable of 100% strain recovery at a tailorable temperature between 80 and 130 °C.[122] As a demonstration they made a Veriflex airfoil capable of deploying from a rolled configuration, as shown in Fig. 7, and investigated it as a wing skin for a chordwise morphing airfoil. The SMP's ability to change modulus allows the wing skin to rigidize. Heating was accomplished through embedded nichrome wires, but various filler materials were also evaluated.[121] Wire spring heating elements have also been used, which allow larger strains without delamination.[123] Toughness, tear strength, and Young's modulus of SMP airfoil skin have been enhanced by adding a 20% volume fraction of elastic fibers.[124] A morphing wing concept made entirely out of SMP and SMP composites has been investigated, and the elastic steel reinforced SMP composite deployed the fastest at a sluggish 5 s.[125] Others have demonstrated sweep changes up to 25° using a carbon-fiber-reinforced SMP composite hinge though full recovery took 8–10 min of heating,[126] which is longer than the vast majority of projectile flight times.

Fig. 7 Veriflex airfoil deploying from rolled state (Reprinted with permission from Reed et al.[121])

Carbon-fiber-wound SMP composite tubes have been studied, demonstrating an impressive modulus ratio of 79.[127] Later improvements imbedded SMP composite tubes in a silicon matrix as fluidic muscles to create a variable stiffness morphing skin. This hybrid concept used thermally regulated water to heat the tube, resulting in modulus changes of 4–230 MPa.[128]

A self-deploying truss consisting of SMP foam spars between two bistable carbon fiber tape springs used the SMP to increase the buckling resistance and as a locking mechanism pre- and postdeployment. The tape springs provided the energy for deployment, axial stiffness, stability, and reduced the storage space.[129]

Temporal SMPs use covalent crosslinks for elastic energy storage and temporary hydrogen bonds to regulate the programmable, sequential deployment. The material is easily programmed by holding a deformed shape. The longer the shape is held, the slower it takes to recover, typically on the order of seconds to minutes.[130] Since most projectiles follow a well-known trajectory, temporal SMPs might be used to augment other structures during each phase of flight, but long-term storage could pose problems.

DEs exhibit large reversible elastic deformations in the presence of an electric field.[131] They benefit from high energy density, short response time, high electromechanical conversion efficiency, low weight, and flexibility, but are limited by their low force and robustness. The larger electric field, the larger the displacement, but these fields can approach the dielectric breakdown voltage resulting in limited cycle life. DEs flatten and increase in area in the presence of an electric field as a result of the Maxwell stress effect.[132]

Barbu et al.[133] investigated the flow over a DE membrane without prestrain. Results showed that step responses altered the camber of the membrane, which increased lift and delayed stall. DE actuation was also able to cycle between attached and unattached flow conditions.[133]

Commercially available DEs are incredibly limited as actuators, but several techniques have been developed to improve their capability, including polymer blends that increase dielectric permittivity[134] and prestraining the DE.[135,136] Ha et al. combined these techniques by preserving DE prestrain using a functional additive, but this resulted in a stiffer elastomer that limited the electrically induced strain.[135] High permittivity has been shown to decreases the actuation voltage, while a higher shear modulus increases the voltage while reducing the likelihood of snap-through instability.[137] Increases in temperature increase the critical electric field and critical strain values, thereby delaying or eliminating instability.[138]

Force, displacement, and efficiency of DE can be improved by layering active elements along with compliant electrodes. Several methods have been investigated including stacked and helical configurations.[139,140] Carpi et al. created contractile DE actuators by folding a planar DE/electrode sheet into a monolithic structure.[141] These actuators increase in cross-sectional area as they contract. Bending actuators of both 1 and 2 degrees of freedom have been made by combining two or four actuators in antagonistic configurations.[142] Other bending actuators consists of two layers with differing shear moduli, one of which is a dielectric elastomer. When actuated, the DE expands while the opposing layer resists, causing the actuator to bend, with maximum bending occurring when both layers have near-identical shear moduli.[143] In general, these actuators require a large amount of DE to achieve modest forces and displacements, which limits their applicability to projectiles.

Several researchers have investigated DE for bistable actuators. DE-actuated bistable trusses can decrease actuation time but are bulkier than other techniques because of the truss and supporting framework.[132,144,145] Others have used DE as the bistable element itself, yielding 10 times the volumetric energy density. This improved reliability, as fewer DE layers are required, but reduced actuation speed and required constant power to resist viscoelastic forces.[146] Keplinger et al. created a balloon-like bistable DE actuator that increased in area up to 1692% after electrically triggered snap-through instability released the stored mechanical energy.[147]

The low blocking force of active polymers effectively invalidates SMPs and DEs as actuators for projectiles. However, they still could prove useful to augment other concepts as in the pressurized muscle example[128] or selectively change the stiffness in individual regions of truss or cellular structures.

5. Compliant Structures

Compliant structures are monolithic, truss-like structures that rely on elastic deformation of their constituent elements to transmit motion and force. These structures can provide several benefits, including reduced complexity, zero backlash and wear, submicron accuracy, and embedded actuation.[148] These can be easily and affordably built through direct[149] or indirect additive manufacturing.[150]

The most mature compliant morphing wing found in the literature to date was developed by FlexSys, Inc., under contract from NASA and the US Air Force Research Laboratory (AFRL) (Fig. 8). Compliant, seamless flaps were investigated, showing significant performance improvements, including 40% increase in control authority, 75% increase in L/D at AoA, 15% increase in endurance, 33% less actuation force, and 17% lower peak power during a max-g pull-up maneuver, as well as improved flow attachment.[151,152] These early successes led to a full-scale version of the compliant wing replacing traditional flaps on a modified Gulfstream GIII, shown in Fig. 8.[153] After extensive ground-based testing,[154,155] multiple successful flight experiments were conducted.[156] The flaps are capable of –9° upward and +40° downward deflections as well as span-wise twisting up to 30°/s.[157]

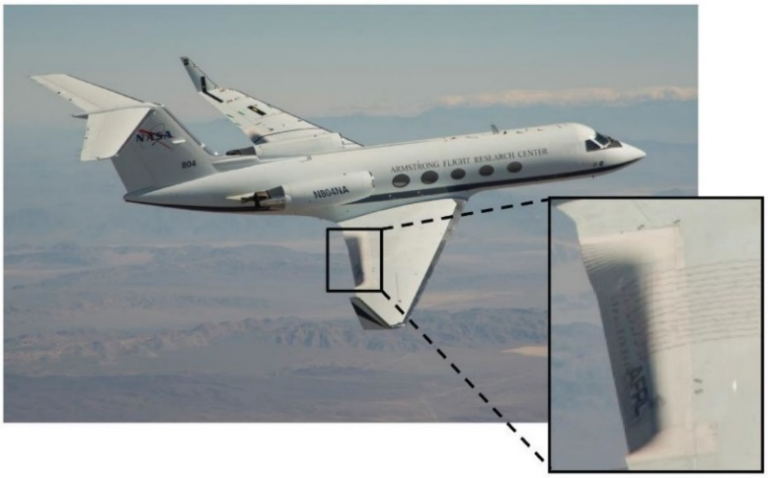

Fig. 8 Adaptive compliant trailing edge flap at 30° deflection during flight experiment (Reprinted with permission from Herrera et al.[155])

The primary challenge when designing compliant structures for morphing applications is selecting the proper topology resulting in the desired motion. Since the design space is poorly understood, global optimization methods such as genetic algorithms have been implemented to determine the required compliant structure necessary for a desired shape change,[158] including variable density,[159] structural

network methods,[160] and modified ground structure methods using the eigenmodes of the stiffness matrix.[161–163]

Compliant structures with piezoelectric beams,[164] SMAs,[165] MFCs,[166] and cable-actuated octahedral trusses[167] have been investigated. Wildschek et al.[168] created a composite trailing edge with independent halves that could morph more than 35° and, if actuated oppositely, provide air braking. Piezoelectricly driven oscillating compliant structures have been used for active flow control[169] similar in function and purpose to pulsed vortex generators.[170–173]

Advances in multimaterial additive manufacturing have allowed for digital materials with tailored mechanical properties within the same part.[174] This can expand the applications of compliant structures that have traditionally relied on a single material.

Compliant structures are very applicable to projectiles and should be considered for morphing modes with low to moderate deflection requirements. While the deflection of compliant structures is substantial, the reliance on elastic deformation prevents them from achieving large deflections. The bandwidth and force are regulated by the input actuator. The impressive camber morphing achieved by FlexSys and their partners is directly applicable to projectiles if the compliant structure is scaled down and driven with a higher bandwidth actuator. Opportunities also exist in leading-edge morphing for improved omnisonic performance.

6. Periodic Cellular Structures

This section covers periodic cellular structures that are repeated, closed-cell structures that exhibit higher global strains than the material properties allow due to the topology of the unit cell. These structures can exceed 10 times more global strain than the maximum strain of the virgin material without locally yielding.[175–177] Such structures have shown auxetic and zero Poisson's ratio (ZPR) properties as well as snap-through and/or bistable behavior. Positive and negative Poisson's ratios, however, exhibit unwanted anticlastic and synclastic curvatures,[178,179] which can addressed by cutting slots to reduce stiffness[180] as well as changes in cell geometry, creating 2-D ZPR structures.[181]

ZPR structures are attractive for morphing wings due to their low in-plane stiffness, high strain capacity, and 1-D response. Out-of-plane stiffness can be controlled by cell geometry and can carrying aerodynamic loads by providing skin support.[177] These structures are typically actuated via tension or compression, but shear-morphed cellular structures have also been investigated.[182]

Spanwise morphing wings capable of doubling in length using ZPR cells and near-zero Poisson's ratio skin have been demonstrated with minimal out of plane deflections.[183,184] Chordwise morphing structures have been passively actuated by rotor centrifugal force using a counterweight[176] or spring (spanwise and chordwise morphing using ZPR structures are shown in Fig. 9).[185] Two independent, antagonistic chordwise morphing structures can achieve camber morphing[186] and, if actuated simultaneously, chordwise morphing. Camber morphing of an auxetic hexachiral airfoil has been investigated to passively change camber proportional to free-stream velocity[187] and has proven successful in wind tunnel experiments.[188]

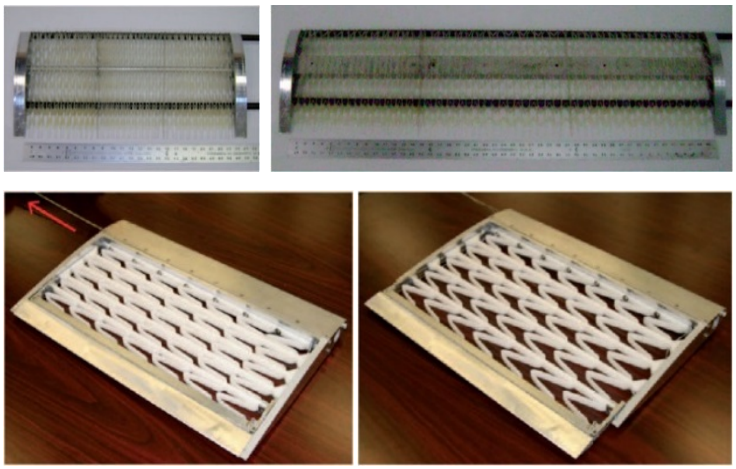

Fig. 9 (top) 1-D spanwise morphing with a ZPR structure and (bottom) 1-D chordwise morphing with a ZPR structure (Reprinted with permission from [top] Vocke et al.[184] and [bottom] Barbarino et al.[176])

SMAs have also been incorporated into cellular structures to take advantage of their large strain recovery potential[189,190] as well as thermally activated morphing.[191] Pressure-actuated cellular structures use inflatable inserts or sealed cell chambers and have demonstrated high blocking force, large achievable strains, and high-frequency actuation.[192–197] Topology optimization has also been applied to individual cells for morphing applications.[198]

Bistable cellular structures have also been investigated for tunable stiffness, high strains, and energy absorption.[199–201] The stress–strain curves can be tailored based on the geometry of the unit cell resulting in monolithic, bistable, or snap-through instabilities as well as incremental and programmable changes in stiffness.[199,202,203] The velocity of the shape transition wave for bistable elements is dependent on the precompression and amplitude of the input force.[204] Exotic cell geometries including polygons[205–207] and arrays of variable holes[208] have shown auxetic and hysteretic programmability.[209]

Bandwidth and force of periodic cellular structures are governed by the input actuator identical to compliant structures. The large deflections of these structures

make them ideal for spanwise, chordwise, and camber morphing of projectile surfaces. ZPR structures are particular interest because they allow the designer to isolate morphing modes relative to one another.

6. Bistable Structures

Bistable structures have two stable states that can switch, given some energy input, and require no energy to maintain a state. These structures are capable of large deformations and high bandwidth resulting from internal material stresses.[210]

Camber morphing concepts using bistable plates have been investigated[211,212] and wind tunnel experiments demonstrated 10° of morphing in under 50 ms.[213] Others have noted the temperature dependency on bistable modes[214] with a complete loss of bistability possible.[211] Prestressing select fibers in a composite during manufacturing can achieve bistability without relying on thermal stresses.[215]

Chordwise morphing[211] as well as a passively actuated dihedral morphing winglet[216] have also been studied along with bistable twisting I-beams[217,218] and spars.[219] I-beams are attractive due to their high bending stiffness, low torsional stiffness, and compliance. Wind tunnel experiments showed zero torsional stiffness bistable I-beams could twist a wind turbine blade ±5°.[220]

A variable-sweep wing box, shown in Fig. 10, consisted of two curved interconnected bistable spars and could be tailored to snap based on their curvature and asymmetric fiber layup.[221] This technique might be applicable to omnisonic projectiles where supersonic drag can be used to passively actuate wing sweep.

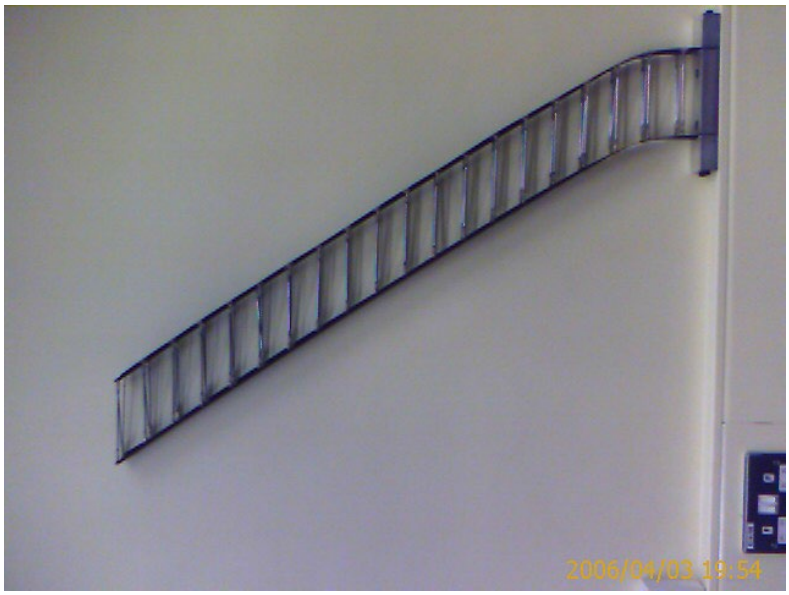

Fig. 10 Wing box in swept state (Reprinted with permission from Mattioni et al.[221])

MFC patches[222–224] and SMA[225,226] wires have been used to trigger snap through in bistable composites at frequencies up to 10 Hz. Arrieta et al. actuated MFC patches at the composite resonant frequency to reduce the force requirement[227] and validated the concept in wind tunnel experiments.[228]

Bistable composite shells that have a coiled cylindrical state and a curved longitudinal state similar to a tape measure have also been investigated.[229–231] Murphey and Pellegrino investigated neutrally stable tape springs, which are stable throughout the rolling/unrolling process, and investigated SMA and piezoelectric actuators to deploy and retract.[230]

Dai et al. created multistable lattice structures from bistable laminates exhibiting 2^N stable modes, highlighting the potential for semi-continuous morphing using discrete bistable composites formed into a cellular structure.[232] Others showed that multistable composites were possible within a single laminate by including local reinforcement strips of fiber[233] or metal.[234]

Bistable structures can be useful for projectiles where discrete changes are desired, such as deployment of control surfaces or Mach regime tuning. However, the discrete, abrupt, and uncontrolled transition of bistable structures limit their implementation where a smooth transition is required. One of the best applications of bistable structures could be deploying and locking surfaces at launch by using the launch acceleration as the input energy. The structure could be tailored to the gun launch acceleration because it is 1–2 orders of magnitude more than that experienced during rough handling. This would allow deployable surfaces to remain locked in both their deployed and stowed state without relying on springs, which are prone to fatigue and creep during years of storage. Structures with a coiled state are also of particular interest because of the cylindrical constraints imposed by the barrel.

9. Inflatable Structures

Inflatable structures provide substantial benefits for aerial vehicles, such as reduced volume, weight, cost, and ease of use. Inflatable structures and wings have been investigated since the 1930s,[235] with the first successful vehicle flown in 1959.[236]

Several gun-launched vehicles have incorporated inflatable structures, one of which, shown in Fig. 11 on a FASM/QuickLook unmanned aerial vehicle (UAV), had inflatable wings and stabilizers that deployed near apogee while the vehicle was traveling at 113 ft/s (34 m/s).[237] Inflatable stabilization fins were also investigated for 250- and 500-lb bomb applications up to Mach 1.2 with inflation occurring in under 150 ms at 200 psi.[238]

Fig. 11 FASM/QuickLook UAV ground testing of inflatable structures (Reprinted with permission from Smith et al.[237])

The main drawbacks with inflatable wings is their load carrying capacity because they rely on the tension in the walls of the structure. As loading increases, the wings begin to wrinkle, then buckle, but can recover once the loading decreases.[239] Other drawbacks include gas leakage and aeroelasticity. The degree to which this behavior influences flight performance depends on the internal pressure, dynamic pressure, and wing geometry.[240] Rendall et al. concluded that aeroelastic phenomenon is dominated by vortex shedding and flow-induced vibration at higher airspeeds and AoA.[240]

To address these drawbacks, researchers have investigated methods for improving the stiffness of inflatable structures without compromising packing efficiency. Increasing the inflation pressure will increase the stiffness, but this can exacerbate leaks and increase reliance on inflation gas. Others have used compliant foam fillers to increase the stiffness,[241] but resin curing methods such as UV and reactive inflation gas rigidization remain the most promising. Once this resin is cured, the wings no longer require the inflation gas for structural stability.[238] Simpson et al. demonstrated ground-based and high-altitude curing of a rigidizable inflatable wing using solar-derived UV radiation[242–247] The inflatable, rigidizable UAV wings cured on the order of minutes and were subsequently vented to the atmosphere to demonstrate their structural integrity.[248] Flexible UV LED arrays have been investigated as an alternative to solar-derived radiation and decreased the cure time to 30 s.[249] However, this is still too slow for projectile applications, so reactive inflation gas curing might be the preferred method in this case.

The flexible nature of inflatable airfoils have enabled morphing concepts to be applied such as twisting and camber morphing.[239,244,246,247] Simpson et al. used high-torque servos and SMAs to morph an inflatable wing. While the servos could morph the wing considerably, they added rigid components that could hinder packaging while the SMAs produced only 3° twist.[246,250]

Inflatable structures are attractive for projectiles because of their small storage and large overall shape change; however, they are greatly limited by their load carrying capacity. The "walls" of the inflated spare act like an I-beam carrying the wing load, but as the loading increases, the inflation pressure can no longer maintain the "I" shape, which begins to buckle, resulting in exponentially decreasing strength and stiffness. This has led to thicker, less efficient, exclusively subsonic airfoils for projectile applications. A hybrid concept may be more appropriate, wherein a rigid material supports the load and the inflatable structure maintains the aerodynamic profile thus exchanging packing efficiency for load capacity.

10. Pressurized Artificial Muscles

The actuators highlighted in this section have been called many things in the literature: McKibben actuators, pneumatic/pressurized artificial muscles, rubber muscle actuator, fluid actuator, fluid-driven tension actuator, rubbertuator, tension actuator, axially contractible actuator, braided artificial muscle, fluidic muscle, and flexible matrix composite (FMC) structures. FMCs have also been used to describe anisotropic skin composite made of unidirectional fibers imbedded in an elastomer matrix.[251,252] For simplicity, all actuators will hereafter be referred to as pressurized artificial muscles (PAMs), as this term can be applied to both pneumatic and hydraulic applications. PAMs are contractile actuators consisting of an elastomer liner surrounded by high-tensile-strength fibers. As a working fluid pressurizes the PAM, the elastomer expands radially and the fibers transfer the radial expansion to tension. These actuators have many benefits, such as low-cost manufacturing, high force-to-weight ratio, moderate bandwidth, soft and compliant, chemical and thermal resistance, lack of moving parts, misalignment tolerance, and strains up to 40%.[253] Some of the drawback are reduced service life due to fiber friction, nonlinear response, and hysteresis.

PAMs were first patented in 1940 as a method for breaking down coal,[254] but it was not until 1949 that they were patented as actuators.[255] The Bridgestone Corporation patented and commercialized their PAM for robotic arms in 1986.[256,257] The Shadow Robot Company incorporated 40 PAMs into a commercially available dexterous robotic hand.[258,259] Festo[260,261]addressed the cycle life problem of PAMs by embedding the braided sleeve in the elastomer membrane such that the fibers never interfere, thus reducing wear, friction, and heat. These PAMs have a service life of 100,000–10,000,000 cycles and cycle rates up to 150 Hz for vibratory applications.[260,261]

Pleated PAMs (PPAMs), shown in Fig. 12, consist of axially oriented fibers eliminating fiber interactions, reducing operating pressure, and increasing

deflection up to 40% by taking advantage of the unfurling pleats.[262] Antagonistic pairs of PPAM actuators have been used for movement and stiffness control of robotic joints.[263] A single long PPAM can be segmented by retention rings to limit radial expansion with a slight decrease in deflection but without compromising force.[264,265] Nonpleated PAMs with straight fibers have also been investigated and show similar improvements.[266–268] Researchers in Japan addressed the contraction limitations of straight-fiber PAMs by using four pairs of actuators in series to maximize the contraction per unit length.[269]

Fig. 12 PPAM in relaxed and contracted states (Reprinted with permission from Verrelst et al.[263])

PAMs have been incorporated into morphing wing sections, resulting in leading- and trailing-edge deformations of 14° and 13°, respectively, at 40 psi, generating a 150-lb blocking force.[270] Others have investigated PAMs for actuating a span-wise morphing truss[183,252] as well as using two antagonistic pairs for conventional flap actuation. At 0.1 Hz, ±40° was achievable but dropped to ±5° at 25 Hz due to insufficient flow rates in the system.[271] Further refinement demonstrated ±20° flap deflection up to 24 Hz.[272] A similar approach was applied to flap control of a rotor blade with high control authority observed up to 35 Hz.[253]

Building on the work of Chou and Hannaford,[273] Davis et al. modeled PAMs as analogous to electrical systems, wherein valves and piping were modeled as resistors, actuator volume corresponded to capacitance, and mass flow rate corresponded to current.[274] This led to a novel revelation that PAM bandwidth could be improved by incorporating a filler to decrease PAM volume without sacrificing force. Granular, solid, and liquid fillers were investigated with peak bandwidth increases of 50%, 250%, and nearly 400%, respectively.[274]

Multiple PAMs can also be incorporated to form anisotropic actuated panels that can contract, bend, and twist. PAMs embedded in an elastomer matrix store some of the strain energy in the matrix, which negatively affects overall force and, to a lesser extent, displacement.[275] Complex behavior such as bending and twisting is possible with multiple rows and columns.[276–278] Peel et al. manufactured and validated a 2 × 4 PAM panel demonstrating their morphing potential, as shown in Fig. 13a.[279] Panels with rigid reinforcements selectively applied to one side increased the overall bending effectiveness (Fig. 13b).[280]

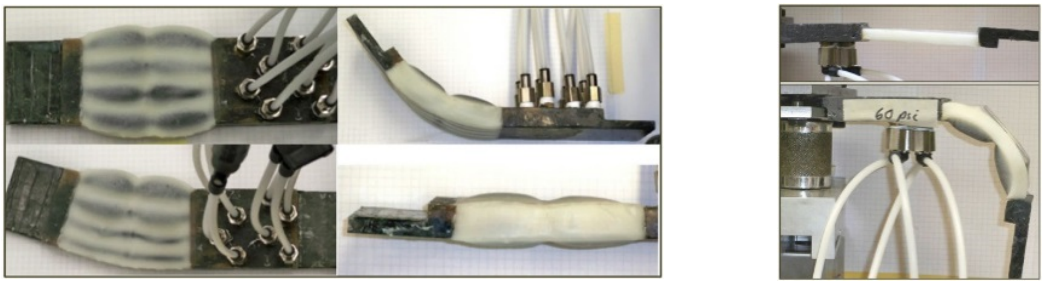

(a) (b)

Fig. 13 a) Clockwise from top left: contraction, out-of-plane bending, twisting, in-plane bending, and b) PAM reinforced for bending (Reprinted with permission from Peel et al.[279])

Self-sensing PAMs have been made by incorporating continuous insulated copper wire into the braid,[280] eutectic gallium indium (eGaIn) microchannels,[281] and DEs as a capacitive sensor.[282,283]

Another unique property of PAMs is their variable stiffness capabilities. PAMs with valve control have demonstrated modulus ratios up to 56 times with ratios over 100 being theoretically possible.[284]

High force, moderate deflection, and moderate bandwidth make PAMs attractive for projectiles. The hysteresis and nonlinear response can be addressed through feedback mechanisms. A set of PAMs could be used as the actuator in a supersonic bending body projectile concept currently being researched.[285,286] PAMs would have an advantage over piezoelectric actuators in this case because of the increased deflection. A wing containing a matrix of PAMs similar to Fig. 13 is also interesting because the wing could be wrapped around the body, rigidized in flight, and morph in several way.

11. Soft Actuators

The emerging field of soft robotics offers new techniques that could be exploited for airframe morphing. Elastomeric actuators come in several forms, including the PAMs discussed previously, but actuators in this section are not limited to uniform braided sleeves or pure contraction. Many of the attributes of soft robotic actuators,

such as low cost, high compliance, high deflection, high force-to-weight ratio, variable stiffness, and ease of manufacturing and implementation, are attractive for precision munitions. The primary drawbacks with all fluid-driven actuators are g-hardening of the pneumatic or hydraulic system and the added complexity of such systems. However, the actuators themselves would likely perform well in a shock environment because of their compliant nature.

Researchers at University of Michigan combined multiple fiber layers into one actuator to achieve a greater range of motion, including extension, contraction, twisting, bending, spiraling, or a mixture of these (Fig. 14).[287,288] The design of these actuators was simplified by using a motion predicting tool without the need for finite-element analysis.[289] When combined in parallel configurations, an even wider range of programmable motion can be achieved.[290,291] If a single family of same-handed helical fibers is used, the actuator contracts and twists.[292] Faudzi et al. combined different braid angles on each hemisphere of a cylindrical soft actuator to produce different degrees of bending.[293] Others used conformal sleeves to mechanically program the output response of soft actuators.[294]

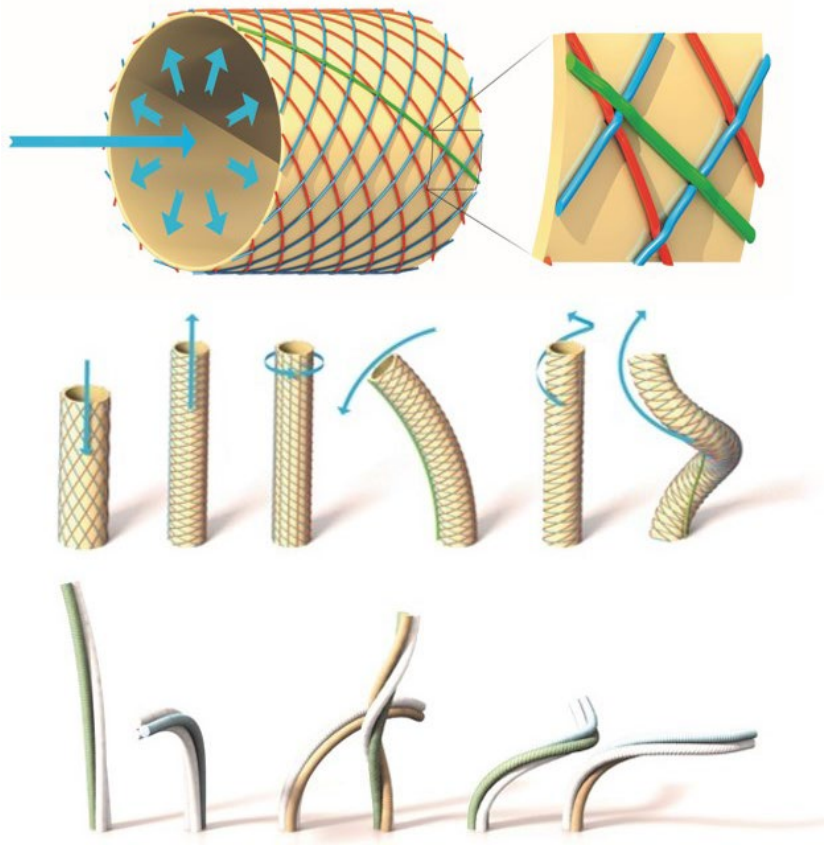

Fig. 14 (top) Multilayered soft actuator; (middle) contracting, extending, spinning, bending, twisting, and spiraling motion as a result of different fiber orientations; and (bottom) resulting motion from three such actuators in parallel (gray actuators are at rest). (Reprinted from Kota [2014]; image courtesy of Bryan Christie Design)

Another class of soft actuators, called pneumatic networks (PneuNets), uses interconnected networks of inflatable channels combined with an inextensible, shear-limiting layer resulting in bending when pressurized. If two actuators are used in an antagonistic configuration, it could be useful for bidirectional camber morphing.

Mosadegh et al. showed how inflation rate, morphology, and material properties impact bandwidth performance and were able to achieve full actuation in 50 ms at 345 kPa. A 4-Hz actuation frequency was demonstrated including a 200-ms venting period between cycles.[295,296] Pleated, 3-D printed PneuNet was able to sweep approximately 180° with a period less than 70 ms (>14 Hz).[297] This kind of bandwidth is within the range necessary for active control of precision munitions. Faster actuation has been achieved by combusting the inflation gas within the soft actuator.[298–300] However, control of the intermediate shapes and velocities would be required for most morphing applications.

An origami approach to folding soft pneumatic membranes can achieve a wide range of motions and anisotropic responses as well as lift loads up to 120 times the actuator weight. Metal foil can act as the shear-limiting layer, creating electrical circuits within the actuator.[301] Copper tape was used in conjunction with eGaIn to determine the shape and surface deformation of elastomer membranes.[302]

Miniature soft actuators are of particular interest to projectile designers given the relatively small size of projectiles. A 2-mm-wide miniature PneuNet used positive and negative pressures to achieved bidirectional actuation.[303] Likewise, fiber-reinforced actuators as small as 1 mm used three independently actuated internal chambers for pitch, yaw, and extension.[304]

The force of soft actuators is regulated by the operating pressure, while bandwidth is regulated by the flow rate, valve speed, and distance. While soft actuators are a new field of research, there are applications to projectiles. Camber morphing with variable stiffness can be achieved using two antagonistic pairs of PneuNets shaped like a trailing edge. Furthermore, the actuators in Fig. 14 could be used as a rigidizable spar capable of omnidirectional bending.

11. Conclusion

This survey report analyzed the literature on smart materials, morphology-dependent structures, and fluid-driven actuators such as SMAs, piezoelectric actuators, MFCs, active polymers, compliant structures, periodic cellular structures, bistable composites, inflatable structures, PAMs, and soft actuators as

well as their applications to projectiles. Some munition examples existed with promising results but have yet to be fielded.

Upon review, these technologies can be classified into two categories based on their applicability to projectile morphing: primary actuators and augmenting technologies. Primary actuators are those that have the deflection, force, and bandwidth to drive a specific morphing mode, while augmenting technologies can enhance the performance of the system but lack the requirements of a primary actuator. Airfoil profile morphing has low actuator demands because of the deceleration time between Mach regimes. Similarly, spanwise and chordwise morphing have low-bandwidth requirements, but large changes in span are desirable for range extension. The deceleration during flight reduces the aero loads and allows for these large changes without inducing aeroelastic instabilities. Camber morphing and twisting have the highest requirements, as this is the primary maneuver method. Sweep can be changed slowly across Mach regimes, but with a higher-bandwidth actuator, sweep could be used for improved maneuverability.

SMAs have high force but low displacement and bandwidth. Therefore, they can only be used as a primary actuator for profile morphing or—with a long enough element—spanwise, chordwise, or sweep morphing. SMAs lack the required bandwidth for camber morphing for most projectile applications. Active cooling such as liquid immersion or thermoelectric cooling are impractical, but thin-film SMAs with sufficiently low thermal mass might be applicable to small-caliber projectiles; however, the bandwidth demands increase for these typically spin-stabilized rounds. SMAs could be incorporated into composites for hypersonic vehicles, but the transient response could prove problematic. Thermoregulation is key if this concept were to be attempted because SMAs lose their memory at high temperatures.

Piezoelectric actuators have been used in munitions, some of which have been shock qualified up to 17,700 g's. The high bandwidth and blocking force is what makes them attractive, but clever amplification schemes are required to make them usable for most projectile applications. Their brittleness poses a challenge during gun launch as well as the long length required to generate modest deflections. However, these remain one of the most attractive primary actuator technologies discussed in this report and continue to be investigated for projectile applications.

MFCs have been thoroughly investigated for use in projectiles and have been found wanting due to a lack of actuator authority. However, they still might be able to augment other systems by adding some small displacement, augmenting stiffness, or triggering snap-through instabilities. The ease of implantation, use, and high

bandwidth are still attractive properties, but MFCs should not be considered a primary actuator for projectile concepts.

The low force, bandwidth, and robustness of active polymer materials limit their application in projectiles; however, their high strain potential makes them good candidates for airfoil skins. One of the best opportunities is augmenting soft actuators or PAM concepts to increase modulus ratios and variable stiffness properties. If placed selectively, these materials can augment individual regions within pneumatic networks, PAMs, cellular structures, or compliant mechanisms. One of the benefits of active polymers is their RF transparency, which will enhance the projectiles' stealth capabilities. However, thermal cycling in a storage bunker could limit shelf life.

Compliant structures are very attractive because their bandwidth, deflection, and force are limited by the driving actuator and material selection. Cost could be a limiting factor, but additive manufacturing technologies could help in this regard. The morphing flaps developed by NASA, AFRL, and FlexSys, Inc., are encouraging, but would need to be much faster and smaller for projectile applications. Compliant structures could be useful for passive profile morphing between supersonic and subsonic Mach regimes as the aero loads differ greatly and the required deflection is small. They are poor candidates where very large deflections are desired, such as spanwise morphing, but they could work for sweeping wings, as the angular deflections are relatively small. Their monolithic nature presents fewer survivability problems than similar linkage-based structures.

Periodic cellular structures are attractive because they are capable of very large global strains without exceeding local material limits. ZPR structures specifically are very useful because of their 1-D response, particularly for hybrid concepts such as a spanwise morphing ZPR structure with morphing rib segments. One of their best uses for projectiles is as a skin support. Structures incorporating inflatable tubes are also attractive due to their high load-carrying potential and variable stiffness as well as, if selectively actuated, profile morphing potential. Bistable or multistable cellular structures are an interesting technology for projectiles that do not re-enter higher Mach regimes postapogee, as the bistable structure can generate large deformations having to return to its original shape. Bandwidth of cellular structures appears dependent on the driving actuator.

Bistable composites could be used as a primary actuator or to enhance the packaging of other airfoil concepts, particularly using coiled configurations given the constraints imposed by gun barrels. If combined with an inflatable structure, a coiled bistable structure could provide support and space-efficient storage. One of their drawbacks as a primary actuator is their inability to control intermediate

shapes; however, their high bandwidth and force can be released if provided enough activation energy. Concepts where a bistable composite airfoil can quickly toggle between positive and negative camber could result in high maneuverability by quickly inverting the sign of the lift vector, but an additional neutral camber angle would be more desirable to minimize unnecessary drag. Other useful concepts include sequentially increasing span as the projectile decelerates or snapping between different airfoil profiles. Bistable composites could be useful in deploying super-caliber surfaces at launch, wherein gun launch provides the activation energy released at muzzle exit. Moisture and temperature dependency are of particular concern for projectiles, as they are typically stored for up to decades at a time. However, temperature-dependent stability might be exploited for shape optimization between hypersonic and high-supersonic Mach regimes where large temperature variations exist.

Inflatable airfoils are attractive due to their packing efficiency, low radar cross section, and extreme shape changes but are limited by their web strength. Other drawbacks include the need for a gas generator or storage tank, but it might be possible to capture and reuse the propellant gas at launch. The high temperature could damage the membrane but the corrosive nature of these gases are not a major concern given the time of flight. A full pneumatics system is not required because the wings are only inflated once. While inflatable airfoils have been applied to subsonic projectiles, the wings will perform worse at higher Mach numbers and loads, as airfoil thickness increases with load. A hybrid concept might be more appropriate where a rigid or rigidizable material replaces the web supporting the wing load while the inflation gas maintains the airfoil profile. This limits the space-saving benefits but should be able to sustain higher loads, reduce the reliance on the inflation gas, and enable thinner, more-efficient airfoils. Since projectiles are typically operating at higher airspeeds than those presented, flow-induced vibration could pose a major challenge in incorporating inflatable structures into munitions. Rigidizable airfoil concepts are only applicable to projectiles with long flights and would probably need to rigidize on the order of seconds to be effective.

PAMs are attractive due to their very high force and deflection. The primary downside is the need for a g-hardened pneumatic or hydraulic system, which adds an additional system not typically used on precision-guided projectiles. The bandwidth of PAMs is dependent on the flow rate through the system that is in turn dependent on orifice size, distance, PAM material, and pressure. Bandwidths higher than 10 Hz have been reported in the literature, sufficient for active control of most projectiles. PAM panels are an attractive concept, as the entire wing can be wrapped around the body, minimizing the space claim and then rigidized in flight. PAMs can also be used as a variable stiffness spar as part of a hybrid design.

The field of soft robotics is young but shows promise as primary actuators for projectile applications. The soft, compliant nature of the actuators will probably survive under high-g accelerations if sufficiently restrained to prevent tearing. They can also be squeezed into irregularly shaped cavities, which provides more options for projectile designers. If these fluid-driven actuators can modulate their internal pressure they can modulate their stiffness, which is particularly attractive for projectiles transitioning through several Mach regimes. Soft actuators benefit from high displacement and blocking force, which scales with pressure. The high force-to-weight ratios of these actuators could prove useful as inflatable spars capable of omnidirectional bending or wing tip actuation. The primary drawbacks are the requirement for a g-hardened pneumatics system and the actuators' bandwidth, which is dependent on orifice size, pressure, solenoid speed, distance, and material selection. However, acceptable bandwidths have been found in the literature. The elastomer materials used have a low radar cross section, which enhances the survivability of the munition against CRAM threats and makes it harder to detect by potentially evasive targets.

Overall, all the technologies investigated could be useful for next-generation morphing projectiles in some fashion. These concepts present a radical transformation in projectile capabilities with the potential to revolutionize the way projectiles are used in the battlefield. Further research will be needed to explore the more promising concepts, but the best opportunities might lie in hybrid concepts that can take advantage of the unique benefits of each technology.

12. References

1. Fresconi F, Celmins I, Ilg M, Maley J. Projectile roll dynamics and control with a low-cost maneuver system. Journal of Spacecraft and Rockets. 2014;51(2):624–627.

2. Fresconi F, Celmins I, Fairfax L. Optimal parameters for maneuverability of affordable precision munitions. Presented at the 50th AIAA Aerospace Sciences Meeting; 2012 Jan; Nashville, TN.

3. Abbott I, von Doenhoff A. Theory of wing sections, including a summary of airfoil data. Chelmsford (MA): Courier Corporation; 1959. p. 6–8.

4. Barbarino S, Flores ES, Ajaj R, Dayyani I, Friswell M. A review on shape memory alloys with applications to morphing aircraft. Smart Materials Structures. 2014;23:063001.

5. Hartl DJ, Lagoudas DC. Aerospace applications of shape memory alloys. Proceedings of the Institution of Mechanical Engineers, Part G: Journal of Aerospace Engineering. 2007;221:535–552.

6. Perkins J. Shape memory effects in alloys. New York (NY): Plenum Press; 1975.

7. Buehler WJ, Gilfrich JV, Wiley RC. Effect of low-temperature phase changes on the mechanical properties of alloys near composition TiNi. Journal of Applied Physics. 1963;34(5):1475–1477.

8. Nitinol Devices and Components, Inc. [accessed 2015 Oct 23]. https://www.nitinol.com/.

9. Dynalloy, Inc. [acccessed 2015 Oct 23]. http://www.dynalloy.com/.

10. Martin CA, Hallam, BJ, Flanagan JF, Bartley-Cho JD. Smart materials and structures – smart wing phase 1 final report. Wright Patterson AFB (OH): Air Vehicles Directorate, Air Force Research Laboratory, Air Force Material Command; 1999.

11. Jardine AP, Bartley-Cho JD, Flanagan JF. Improved design and performance of the SMA torque tube for the smart wing program. Presented at the SPIE Conference on Industrial and Commercial Applications of Smart Structures Technologies; 1999; Newport Beach, CA.

12. Swei S S-M, Nguyen NT. Aeroelastic wing shaping control subject to actuation constraints. Presented at the 55th AIAA/ASMe/ASCE/AHS/SC Structures, Structural Dynamics, and Materials Conference; 2014 Jan 13–17; National Harbor, MD.

13. Icardi U, Ferrero L. Preliminary study of an adaptive wing. Materials and Design. 2009;30:4200–4210.

14. Sofla AY, Elzey DM, Wadley HN. An antagonistic flexural unit cell for design of shape morphing structures. Proceedings of ASME International Mechanical Engineering Congress and Exposition; 2004 Nov 13–19; Anaheim, CA.

15. Elzey DM, Sofla AY, Wadley HN. A shape memory-based multifunctional structural actuator panel. International Journal of Solids and Structures. 2005;42:1943–1955.

16. Sofla AY, Elzey DM, Wadley HN. Two-way antagonistic shape actuation based on the one-way shape memory effect. Journal of Intelligent Material Systems and Structures. 2008;19:1017–1027.

17. Leal PB, Petterson R, Hartl DJ. Design optimization toward a shape memory alloy-based bio-inspired morphing wing. Presented at the 25th AIAA/AHS Adaptive Structures Conference; 2017 Jan 9–13; Grapevine, TX.

18. Kudva JN, Martin CA, Scherer LB, Jardine AP, McGowan AR, Lake RC, Sendeckyj GP, Sanders BP. Overview of the DARPA/AFRL/NASA smart wing program. Presented at the SPIE Conference on Industrial and Commercial Applications of Smart Structures Technologies; 1999; Newport Beach, CA.

19. Martin CA, Bartley-Cho JD, Flanagan JS, Carpenter BF. Design and fabrication of smart wing wind tunnel model and SMA control surfaces. Presented at the SPIE Conference on Industrial and Commercial Applications of Smart Structures Technologies; 1999; Newport Beach, CA.

20. Elzey DM, Sofla AY, Wadley HN. A bio-inspired, high-authority actuator for shape morphing structures. Proceedings of SPIE: Smart Structures and Materials. 2003;5053:92–100.

21. Sofla AY, Elzey DM, Wadley HN. Cyclic degradation of antagonistic shape memory actuated structures. Smart Materials and Structures. 2008;17(2):1–6.

22. Rediniotis OK, Wilson LN, Lagoudas DC, Khan MM. Development of a shape-memory-alloy actuated biomimetic hydrofoil. Journal of Intelligent Material Systems and Structures. 2002;13:35–49.

23. Garner LJ, Wilson LN, Lagoudas DC, Rediniotis OK. Development of a shape-memory-alloy actuated biomimetic vehicle. Smart Materials and Structures. 2000;9(5):673-683.

24. Heyland DR, Sachau HD, Strohmeyer D, Voss R. The adaptive wing project (DLR): survey on targets and recent results from active/adaptive structures viewpoint. Presented at the 10th International Conference on Adaptive Structures and Technologies; 1999; Paris, France.

25. Bauer C, Martin W, Siegling HF. An adaptive composite structure to control the sonic shock of transport aircraft wings. Proceedings of the 4th European Conference on Smart Structures and Materials and 2nd MIMR Conference; 1998; Harrogate, UK.

26. Georges T, Brailovski V, Coutu D, Terriault P. Design diagram for linear SMA actuators integrated in a morphing wing structure. Proceedings of the International Conference on Shape Memory and Superelastic Technologies; 2007 Dec 3–5; Tsukuba, Japan. Materials Park (OH): ASM International; c2008.

27. Coutu D, Brailovski V, Terriault P. Optimized design of an active extrados structure for an experimental morphing laminar wing. Aerospace Science and Technology. 2010;14(7):451–458.

28. Popov AV, Labib M, Fays J, Botez RM. Closed-loop control simulations on a morphing wing. Journal of Aircraft. 2008;45(5):1794–1803.

29. Popov AV. Design of an active controller for delaying the transition from laminar flow to turbulent flow over a morphing wing in wind tunnel [dissertation]. [Montreal (Canada)]: École de technologie supérieure; 2010.

30. Dong Y, Boming Z, Jun L. A changeable aerofoil actuated by shape memory alloy springs. Materials Science and Engineering A. 2008;485:243–250.

31. Sofla AYN, Meguid SA, Tan KT, Yeo WK. Shape morphing of aircraft wing: status and challenges. Materials & Design. 2010;31(3):1284–1292.

32. Grant D, Hayward V. Variable structure control of shape memory alloy actuators. IEEE Control Systems. 1997;17(3):80–88.

33. Miga Motor Company [accessed 2015 October 23]. www.migamotors.com.

34. Colorado J, Barrientos A, Rossi C, Breuer KS. Biomechanics of smart wings in a bat robot: morphing wings using SMA actuators. Bioinspiration & Biomimetics. 2012;7(3):036006.

35. Featherstone R, Teh YH. Improving the speed of shape memory alloy actuators by faster electrical heating. Proceedings of the 9th International Symposium Experimental Robotics; 2004 June 18–24; Singapore.

36. Teh YH, Featherstone R. An architecture for fast and accurate control of shape memory alloy actuators. International Journal of Robotics Research. 2008;27(5):595–611.

37. Clark PW, Aiken ID, Kelly JM, Higashino M, Krumme R. Experimental and analytical studies of shape-memory alloy dampers for structural control. Proceedings of the SPIE Smart Structures and Materials Conference; 1995; San Diego, CA.

38. Teh YH. Fast, accurate force and position control of shape memory alloy actuators. Canbeerra (Australia): Australian National University; 2008.

39. Gorbet RB, Russell RA. A novel differential shape memory alloy actuator for position control. Robotica. 1995;13(4):423–430.

40. Gill JJ, Ho K, Carman GP. Three-dimensional thin-film shape memory alloy microactuator with two-way effect. Journal of Microelectromechanical Systems. 2002;11(1):68–77.

41. Loh CS, Yokoi H, Arai T. New shape memory alloy actuator: design and application in the prosthetic hand. Proceedings of the Engineering in Medicine and Biology 27th Annual Conference; 2005; Shanghai, China.

42. Bil C, Massey K, Abdullah EJ. Wing morphing control with shape memory alloy actuators. Journal of Intelligent Material Systems and Structures. 2013;24(7):879–898.

43. Iwanaga H, Tobushi H, Ito H. Basic research on output power characteristics of a shape memory alloy heat engine: twin crank heat engine. JSME International Journal. 1988;31(3):634–637.

44. Taylor PM, Moser A, Creed A. A sixty-four element tactile display using shape memory alloy wires. Displays. 1998;18:163–168.

45. Thrasher MA, Shahin AR, Meckl PH, Jones JD. Thermal cycling of shape memory alloy wires using semiconductor heat pump modules. European Conference on Smart Structures and Materials. 1992;1777:197–200.

46. Bergamasco M, Salsedo F, Dario P. A linear SMA motor as direct-drive robotic actuator. Proceedings of IEEE International Conference on Robotics and Automation; 1989; p. 618–623.

47. Wellman PS, Peine WJ, Favalora G, Howe RD. Mechanical design and control of a high-bandwidth shape memory alloy tactile display. Experimental robotics V. London (UK): Springer-Verlag; 1998; p. 56–66.

48. Knebel AM, Salemi MR, inventors; Shape memory alloy fuel injector small package integral design. Delphi Technologies Inc, assignee. United States patent US 6,318,641. 2001 Nov 20.

49. Krulevitch P. Thin film shape memory alloy microactuators. Journal of Microelectromechanical Systems. 1996;5(4):270–282.

50. Hübler M, Gurka M, Schmeer S, Breuer UP. Performance range of SMA actuator wires and SMA–FRP structure in terms of manufacturing, modeling and actuation. Smart Materials and Structures. 2013;22(9):094002.

51. Barrett RM. Adaptive aerostructures: the first decade of flight on uninhabited aerial vehicles. Smart Structures and Materials; 2004; San Diego, CA.

52. Barrett R, Lee G. Guided bullets: A decade of enabling adaptive materials R&D. Auburn (AL): Auburn University; 2004.

53. Barrett R. 20 years of adaptive aerostructures in flying missiles, munitions and UAVs. Presented at the ASME 2014 Conference on Smart Materials, Adaptive Structures and Intelligent Systems; 2014; Newport, RI.

54. Chee CY, Tong L, Steven GP. A review on the modelling of piezoelectric sensors and actuators incorporated in intelligent structures. Journal of Intelligent Material Systems and Structures. 1998;9(1):3–19.

55. Mossi K, Bryant R. Characterization of piezoelectric actuators for flow control over a wing. Proceedings of the 9th International Conference on New Actuators; 2004; Breman, Germany.

56. Clingman DJ. Development of an aerodynamic synthetic jet actuator based on a piezoceramic buckled beam [MS thesis]. [College Park, (MD)]: University of Maryland; 2006.

57. Massey KC, McMichael J, Warnock T, Hay F. Design and wind tunnel testing of guidance pins for supersonic projectiles. Presented at the 24th Army Sciences Conference; 2005 Nov 29–Dec 2; Orlando, FL.

58. Lovas A, Brown T, Harkins T. Innovative technologies and techniques for in-situ test and evaluation of small caliber munitions. ITEA Journal. 2008;29:29–36.

59. McMichael J, Plostins P, Sahu J, Glezer A, Lovas A, Brown G, Rinehart C. Microadaptive flow control applied to a spinning projectile. Proceedings of the 2nd AIAA Flow Control Conference; 2004 June 28–July 1; Portland, OR.

60. Dynamic Structures & Materials, LLC. Piezo actuators [accessed 20 April 2017]. http://www.dynamic-structures.com/actuators#fpa.

61. Barrett R, Stutts J. Development of a piezoceramic flight control surface actuator for highly compressed munitions. Proceedings of the 39th Structures, Structural Dynamics and Materials Conference; 1998; Long Beach, CA.

62. Barrett R, Stutts J. Modeling, design, and testing of a barrel-launched adaptive munition. Proceedings of Smart Structures and Materials; 1997; San Diego, CA.

63. Barrett RM, Lee GM. Design and testing of piezoelectric flight control actuators for hard-launch munitions. Proceedings of Smart Structures and Materials; 2004; San Diego, CA.

64. Barrett R. Actuation strain decoupling through enhanced directional attachment in plates and aerodynamic surfaces. Proceedings of the European Conference on Smart Structures and Materials; 1992; Glasgow, UK.

65. Barrett R. Active plate and wing research using EDAP elements. Smart Materials and Structures. 1992;1(3):214.

66. Barrett R. Active plate and missile wing development using directionally attached piezoelectric elements. AIAA Journal. 1994;32(3):601–609.

67. Barrett RM, Law D. Design, fabrication, and testing of a new twist-active wing design. Proceedings of the 5th Annual International Symposium on Smart Structures and Materials; 1998; San Diego, CA.

68. Barrett RM. All-moving active aerodynamic surface research. Proceedings of the Symposium on Active Materials and Smart Structures: Society of Engineering Science 31st Annual Meeting; 1995; College Station, TX.

69. Barrett RM, Gross RS, Brozoski FT. Design and testing of a subsonic all-moving adaptive flight control surface. AIAA Journal. 1997;35(7):1217–1219.

70. Barrett R. Active aeroelastic tailoring of an adaptive flexspar stabilator. Smart Materials and Structures. 1996;5(6):723–730.

71. Sahoo D, Cesnik CE. Roll maneuver control of UCAV wing using anisotropic piezoelectric actuators. Proceedings of the 43rd AIAA/ASME/ASCE /AHS/ASC Structures, Structural Dynamics and Materials Conference; 2002; Denver, CO.

72. Cesnik CE, Brown EL. Active warping control of a joined-wing airplane configuration. Proceedings of the 44th AIAA/ASME/ASCE/AHS/ASC Structures, Structural Dynamics, and Material Conference; 2003; Hampton, VA.

73. Chiang YM, Farrey GW, Soukhojak AN. Lead-free high-strain single-crystal piezoelectrics in the alkaline-bismuth-titanate perovskite family. Applied Physics Letters. 1998;73:3683.

74. Lee T, Chopra I. Design of piezostack-driven trailing-edge flap actuator for helicopter rotors. Smart Materials and Structures. 2001;10(1):15–24.

75. Spangler RL. Piezoelectric actuators for helicopter rotor control. Cambridge (MA): Massachusetts Institute of Technology; 1989.

76. Koratkar NA, Chopra I. Wind tunnel testing of a mach-scaled rotor model with trailing-edge flaps. Smart Materials and Structures. 2001;1(1):1–14.

77. Straub FK, Ealey MA, Schetky LM. Application of smart materials to helicopter rotor active control. Proceedings of Smart Structures and Materials; 1997; San Diego, CA.

78. Straub FK, Ngo HT, Anand V, Domzalski DB. Development of a piezoelectric actuator for trailing edge flap control of full scale rotor blades. Smart Materials and Structures. 2001;10(1):25–34.

79. Straub FK, Anand VR, Birchette TS, Lau BH. Smart rotor development and wind tunnel test. Mountain View (CA): NASA; 2009 [accessed 2018 May 29]. https://rotorcraft.arc.nasa .gov/Publications/files/straub_2009_783.pdf.

80. Haertling G, inventor; Research Corporation Technologies, Inc., assignee. Method for making monolithic prestressed ceramic devices. United States patent US 5,471,721. 1995 Dec 5.

81. Haertling GH, inventor. Research Corporation Technologies, Inc., assignee. Monolithic prestressed ceramic devices and method for making same. United States patent US 5,589,725. 1996 Dec 31.

82. Hellbaum RF, Bryant RG, Fox RL, inventors. United States of America, assignee. Thin layer composite unimorph ferroelectric driver and sensor. United States patent US 5,632,841. 1997 May 27.

83. Mossi KM, Bishop RP. Characterization of different types of high-performance THUNDER actuators. Proceedings of Smart Structures and Materials; 1999; Newport Beach, CA.

84. Corporation FI. Brief introduction to THUNDER technology. Norfolk (VA): Face® International Corporation; 2018 [accessed 2016 July 7]. http://www.thunderandlightningpiezos.com/technology/.

85. Pinkerton J, Moses R. A feasibility study to control airfoil shape using THUNDER. Hampton (VA): NASA Langley Research Center; 1997.

86. Eggleston Gea. Morphing aircraft design team. Blacksburg (VA): Virginia Tech Aerospace Engineering Senior Design Project; 2002.

87. Wise SA. Displacement properties of RAINBOW and THUNDER piezoelectric actuators. Sensors and Actuators A: Physical. 1998;69(1):33–38.

88. Dausch DE, Wise SA. Compositional effects on electromechanical degradation of RAINBOW actuators. Hampton, (VA): NASA Langley Research Center; 1998.

89. Vos R, Barrett R. Post-buckled precompressed techniques in adaptive aerostructures: an overview. Journal of Mechanical Design. 2010;132(3):031004.

90. Lesieutre GA, Davis CL. Can a coupling coefficient of a piezoelectric device be higher than those of its active material? Proceedings of Smart Structures and Materials; 1997; San Diego, CA.

91. Lesieutre GA, Davis CL, inventors. Penn State Research Foundation, assignee. Transfer having a coupling coefficient higher than its active material. United States patent US 6,236,143. 2001 May 22.

92. Schwartz RW, Narayanan M. Development of high performance stress-biased actuators through the incorporation of mechanical pre-loads. Sensors and Actuators A: Physical. 2002;101(3):322–331.

93. Schwartz RW, Narayanan M, inventors. Clemson University, assignee. Electroactive apparatus and methods. United States patent US 6,847,155. 2005 Jan 25.

94. Vos R, Breuker RD, Barrett RM, Tiso P. Morphing wing flight control via postbuckled precompressed piezoelectric actuators. Journal of Aircraft. 2007;44(4):1060–1068.

95. Vos R, Barrett R, DeBreuker R, Tiso P. Post-buckled precompressed elements: a new class of control actuators for morphing wing UAVs. Smart Materials and Structures. 2007;16(3):919–926.

96. Barrett R, Vos R, Breuker RD. Post-buckled precompressed subsonic micro-flight control actuators and surfaces. Smart Materials and Structures. 2008;17(5):055011.

97. Vos R, Barrett R. Dynamic elastic-axis shifting: an important enhancement of piezoelectric postbuckled precompressed actuators. AIAA Journal. 2010;48(3):583–590.

98. Barrett RM, Tiso P, inventors. No assignee listed. Actuator. United States patent US 7,898,153. 2011 Mar 1.

99. Barrett R, Vos R. Design, development, and testing of a transonic missile fin employing PBP/DEAS actuators. Proceedings of the 15th International Symposium on Smart Structures and Materials and Nondestructive Evaluation and Health Monitoring; 2008; San Diego, CA.

100. Giannopoulos G, Monreal J, Vantomme J. Snap-through buckling behavior of piezoelectric bimorph beams: I. analytical and numerical modeling. Smart Materials and Structures. 2007;16(4):1148–1157.

101. Giannopoulos G, Monreal J, Vantomme J. Snap-through buckling behavior of piezoelectric bimorph beams: II. experimental verification. Smart Materials and Structures. 2007;16(4):1158–1163.

102. Wilkie WK, Bryant RG, Fox RL, Hellbaum RF, High, JW, Jalink A Jr, Little BD, Mirick PH, inventors. National Aeronautics and Space Administration, assignee. Method of fabricating a piezoelectric composite apparatus. United States patent US 6,629,341. 2003 Oct 7.

103. Smart Material Corp. MFC– Macro-fiber composite. Sarasota (FL): Smart Material Corp; 2018 [accessed 20 Jan 2016]. http://www.smart-material.com/MFC-product-main.html.

104. Bilgen O, Erturk A, Inman DJ. Analytical and experimental characterization of macro-fiber composite actuated thin clamped-free unimorph benders. Journal of Vibration and Acoustics. 2010;132(5):051005.

105. Pankonien A, Inman DJ. Experimental testing of spanwise morphing trailing edge concept. Proceedings of SPIE 8688, Active and Passive Smart Structures and Integrated Systems; 2013; San Diego, CA.

106. Pankonien AM. Smart material wing morphing for unmanned aerial vehicles. [dissertation]. [Ann Arbor (MI)]: University of Michigan; 2015.

107. Prazenica RJ, Daewon K, HEver M, Boutros A, Chan M. Design, characterization, and testing of macro-fiber composite actuators for integration on a fixed-wing UAV. Proceedings of SPIE, Vol 9057, ID 905715; 2014 Apr.

108. Pankonien AM, Inman DJ. Spanwise morphing trailing edge on a finite wing. Proceedings of SPIE. 2015;9431.

109. Pankonien AM, Faria CT, Inman DJ. Synergistic smart morphing aileron. Proceedings of the 54th AIAA/ASME/ASCE/AHS/ASC Structures, Structural Dynamics, and Materials Conference; 2013; Boston, MA.

110. Butt L. Wing morphing design utilizing macro fiber composite smart materials. Proceedings of the 69th Annual Conference of The Society of Allied Weight Engineers; 2010; Virginia Beach, VA.

111. Virginia Tech Wing Morphing Design Team. WMD2010_PROMO_SHORT.wmv. Blacksburg (VA):Virginia Tech; 2010 Oct 6 [accessed 2016 Jan 27]. https://www.youtube.com/watch?v=KxTJBp53nO0.

112. Bilgen O, Kochersberger KB, Inman DJ. An experimental and analytical study of a flow vectoring airfoil via macro-fiber-composite actuators. Proceedings of the 15th International Symposium on Smart Structures and Materials and Nondestructive Evaluation and Health Monitoring; 2008; San Diego, CA.

113. Bilgen O, Kochersberger KB, Inman DJ. Novel, bidirectional, variable-camber airfoil via macro-fiber composite actuators. Journal of Aircraft. 2010;47(1):303–314.

114. Cadogan D, Smith T. Morphing inflatable wing development for compact package unmanned aerial vehicles. Proceedings of the 45th AIAA/ASME/ASCE/AHS/ASC Structures, Structural Dynamics & Materials Conference; 2004; Palm Springs, CA.

115. Debiasi M, Chan WL, Bouremel Y, Yap CY. Application of macro-fiber-composite materials on UAV wings. Proceedings of the Aerospace Technology Seminar; 2013; Singapore.

116. Giddings PF. Piezoelectrically actuated bistable composite laminates for structural morphing [dissertation]. [Bath (UK)]: University of Bath; 2010.

117. Schultz MR, Hyer MW. Snap-through of unsymmetric cross-ply laminates using piezoceramic actuators. Journal of Intelligent Material Systems and Structures. 2003;14(12):795–814.

118. Arters J, Vinson J, Bogetti T, Weinacht P, Drysdale W, Leibowitz M, Rabinovitch O. Preliminary design of piezo-activated composite sandwich fins for projectile maneuverability. Proceedings of the 46th AIAA/ASME/ASCE/AHS/ASC Structures, Structural Dynamics and Materials Conference; 2005; Austin, TX.

119. Hickman A, Vinson J, Bogetti T, Weinacht P, Drysdale W, Rabinovitch O. Continued efforts in the development of piezo-activated composite sandwich fins. Proceedings of the 47th AIAA/ASME/ASCE/AHS/ASC Structures, Structural Dynamics, and Materials Conference; 2006; Newport, RI.

120. Hiltz JA. Shape memory polymers – literature review. Defence Research and Development Atlantic; Dartmouth, Canada; 2002.

121. Reed Jr JL, Hemmelgarn CD, Pelley DM, Havens E. Adaptive wing structures. Proceedings of Smart Structures and Materials: Industrial and Commercial Applications of Smart Structures Technologies; 2005; San Diego, CA.

122. CRG introduces Veriflex® E (Epoxy SMP). San Francisco (CA): Cornerstone Research Group, Inc. (CRG); 2006 Mar 30 [accessed 2016 September 9]. http://www.crgrp.com/news/crg-introduces-veriflex-e-epoxy-smp.

123. Yin W, Fu T, Liu J, Leng J. Structural shape sensing for variable camber wing using FBG sensors. Proceedings of SPIE Smart Structures and Materials: Nondestructive Evaluation and Health Monitoring; 2009; San Diego, CA.

124. Sun J, Liu Y, Leng J. Mechanical properties of shape memory polymer composites enhanced by elastic fibers and their application in variable stiffness morphing skins. Journal of Intelligent Material Systems and Structures. 2015;26(15):2020–2027.

125. Yu K, Yin W, Sun S, Lui Y, Leng J. Design and analysis of morphing wing based on SMP composite. Proceedings of SPIE Smart Structures and Materials: Nondestructive Evaluation and Health Monitoring; 2009; San Diego, CA.

126. Yu Y, Li X, Zhang W, Leng J. Investigation on adaptive wing structure based on shape memory polymer composite hinge. Proceedings of SPIE. 2007;6423.

127. Chen Y, Sun J, Liu Y, Leng J. Variable stiffness property study on shape memory polymer composite tube. Smart Materials and Structures. 2012;21(9):094021.

128. Chen S, Chen Y, Zhang Z, Liu Y, Leng J. Experiment and analysis of morphing skin embedded with shape memory polymer composite tube. Journal of Intelligent Material Systems and Structures. 2013;25(16):2052–2059.

129. Sokolowski,W, Tan S, Pryor M. Lightweight shape memory self-deployable structures for Gossamer applications. Proceedings of the 45th AIAA/ASME/ASCE/AHS/ASC Structures, Structural Dynamics & Materials Conference; 2004; Palm Springs, CA.

130. Hu X, Zhou J, Vatankhah-Vardosfaderani M, Daniel WFM, Li Q, Zhushma AP, Dobrynin AV, Sheiko SS. Programming temporal shapeshifting. Nature Communications. 2016;7:12919.

131. Bar-Cohen Y. Electroactive polymers: current capabilities and challenges. Proceedings of the SPIE 9th Annual International Symposium on Smart Structures and Materials; 2002; San Diego, CA.

132. Plante J-S Dielectric elastomer actuators for binary robotics and mechatronics [thesis]. [Cambridge (MA)]: Massachusetts Institute of Technology; 2006.

133. Barbu IA, de Kat R, Ganapathisubramani B. Aerodynamic step input response of electro-active membrane wings. Proceedings of the 25th AIAA/AHS Adaptive Structures Conference; 2017 Jan 9–13; Grapevine, TX.

134. Carpi F, Gallone G, Galantini F, De Rossi D. Silicone–poly (hexylthiophene) blends as elastomers with enhanced electromechanical transduction properties. Advanced Functional Materials. 2008;18(2):235–241.

135. Ha SM, Yuan W, Pei Q, Pelrine R, Stanford S. Interpenetrating networks of elastomers exhibiting 300% electrically-induced area strain. Smart Materials and Structures. 2007;16(2):S280–S287.

136. Li B, Chen H, Qiang J, Zhou J. A model for conditional polarization of the actuation enhancement of a dielectric elastomer. Soft Matter. 2012;8(2):311–317.

137. Li B, Liu L, Suo Z. Extension limit, polarization saturation, and snap-through instability of dielectric elastomers. International Journal of Smart and Nano Materials. 2011;2(2):59–67.

138. Liu L, Liu W, Li B, Yang K, Li T, Leng J. Thermo-electro-mechanical instability of dielectric elastomers. Smart Materials and Structures. 2011;20(7):075004.

139. Schlaak HF, Jungmann M, Matysek M, Lotz P. Novel multilayer electrostatic solid state actuators with elastic dielectric. Proceedings of Smart Structures and Materials 2005: Electroactive Polymer Actuators and Devices; 2005; San Diego, CA.

140. Carpi F, Migliore A, Serra G, De Rossi D. Helical dielectric elastomer actuators. Smart Materials and Structures. 2005;14(6):1210.

141. Carpi F, Salaris C, De Rossi D. Folded dielectric elastomer actuators. Smart Materials and Structures. 2007;16(2):S300–S305.

142. Carpi F, De Rossi D. Contractile folded dielectric elastomer actuators. Proceedings of SPIE. 2007;6524.

143. Henann DL, Chester SA, Bertoldi K. Modeling of dielectric elastomers: design of actuators and energy harvesting devices. Journal of the Mechanics and Physics of Solids. 2013;61(10):2047–2066.

144. Plante JS, Santer M, Dubowsky S, Pellegrino S. Compliant bistable dielectric elastomer actuators for binary mechatronic systems. Proceedings of the ASME International Design Engineering Technical Conferences and Computers and Information in Engineering Conference; 2005; Long Beach, CA.

145. DeVita LM. An MRI compatible manipulator for prostate cancer detection and treatment [thesis]. [Cambridge (MA)]: Massachusetts Institute of Technology; 2007.

146. Chouinard P, Plante JS. Bistable antagonistic dielectric elastomer actuators for binary robotics and mechatronics. IEEE/ASME Transactions on Mechatronics. 2012;17(5):857–865.

147. Keplinger C, Li T, Baumgartner R, Suo Z, Bauer S. Harnessing snap-through instability in soft dielectrics to achieve giant voltage-triggered deformation. Soft Matter. 2012;8(2):285–288.

148. Kota S. Compliant systems using monolithic mechanisms. Smart Materials Bulletin. 2001 Mar:7–10.

149. Moon SK, Tan YE, Hwang J, Yoon YJ. Application of 3D printing technology for designing light-weight unmanned aerial vehicle wing

structures. International Journal of Precision Engineering and Manufacturing-Green Technology. 2014;1(3):223–228.

150. Tan YE, Moon SK. Inflatable wing design for micro UAVs using indirect 3D printing. Proceedings of the 11th International Conference on Ubiquitous Robots and Ambient Intelligence; 2014; Kuala Lumpur, Malaysia.

151. Kota S, Osborn R, Ervin G, Maric D, Flick P, Paul D. Mission adaptive compliant wing–design, fabrication and flight test. Proceedings of the NATO RTO Applied Vehicle Technology Panel (AVT) Symposium; 2009; Evora, Portugal.

152. Hetrick JA, Osborn R, Kota S, Flick P, Paul D. Flight testing of mission adaptive compliant wing. Proceedings of the 48th AIAA/ASME/ASCE/AHS/ASC Structures, Structural Dynamics, and Materials Conference; 2007 Apr 23–26; Honolulu, HI.

153. Beutel A, ed. NASA tests revolutionary shape changing aircraft flap for the first time. Washington (DC): NASA; 2014 Nov 7 [accessed 2015 Dec 17]. http://www.nasa.gov/press/2014/november/nasa-tests-revolutionary-shape-changing-aircraft-flap-for-the-first-time/.

154. Miller EJ, Lokos WA, Cruz J, Crampton G, Stephens CA. Approach for structurally clearing an adaptive compliant trailing edge flap for flight. Edwards (CA): Armstrong Flight Research Center, NASA; 2015.

155. Herrera CY, Spivey ND, Lung S-f, Ervin G, Flick P. Aeroelastic airworthiness assesment of the adaptive compliant trailing edge flaps. Edwards (CA): Armstrong Flight Research Center, NASA; 2015.

156. Lau S. Wing morphing. Professional Pilot; 2015 Dec 17 [accessed 2015 Dec 17]. http://www.propilotmag.com/archives/2015/April%2015/4 _wingmorphing_p1.html.

157. Tsang K. FlexFoil wing tests peaking. FlexSys; 2015 Jan 5 [accessed 2015 Dec 17]. http://www.flxsys .com/blog/2015/1/5/flexfoil-wing-tests-peaking.

158. De Gaspari A, Ricci S. A two-level approach for the optimal design of morphing wings based on compliant structures. Journal of Intelligent Material Systems and Structures. 2011;22(10):1091–1111.

159. Santer M, Pellegrino S. Topological optimization of compliant adaptive wing structure. AIAA Journal. 2009;47(3):523–534.

160. Santer M, Pellegrino S. Topology optimization of adaptive compliant aircraft wing leading edge. Proceedings of the 48th AIAA/ASME/ASCE/AHS/ASC

Structures, Structural Dynamics, and Materials Conference; 2007; Honolulu, HI.

161. Hasse A, Campanile LF. Design of compliant mechanisms with selective compliance. Smart Materials and Structures. 2009;18(11).

162. Hasse A, Zuest I, Campanile LF. Modal synthesis of belt-rib structures. Proceedings of the Institution of Mechanical Engineers, Part C: Journal of Mechanical Engineering Science. 2011;225(3):722–732.

163. Previtali F, Bleischwitz R, Hasse A, Ermanni P. Compliant morphing wing. Proceedings of the 22nd International Conference on Adaptive Structures and Technologies; 2011 Oct 10–12; Corfu, Greece.

164. Anusonti-Inthra P, Sarjeant R, Frecker M, Gandhi F. Design of a conformable rotor airfoil using distributed piezoelectric actuators. AIAA Journal. 2005;43:1684–1695.

165. Lagoudas DC, Strelec JK, Yen J, Khan MA. Intelligent design optimization of a shape-memory-alloy-actuated reconfigurable wing. Proceedings of SPIE. 2000 Jan 1;3984:338–348.

166. Henry AC, Molinari G, Arrieta AF. Smart morphing wing: optimization of distributed piezoelectric actuation. Proceedings of the 25th AIAA/AHS Adaptive Structures Conference; 2017 Jan 9–13; Grapevine, TX.

167. Ramrakhyani DS, Lesieutre, GA, Frecker M, Bharti S. Aircraft structural morphing using tendon-actuated compliant cellular trusses. Journal of Aircraft. 2005;42(6)1614–1620.

168. Wildschek A, Havar T, Plötner K. An all-composite, all-electric, morphing trailing edge device for flight control on a blended-wing-body airliner. Proceedings of the Institution of Mechanical Engineers, Part G: Journal of Aerospace Engineering. 2010;224(1):1–9.

169. Osborn RF, Kota S, Hetrick JA, Geister DE, Tilmann CP, Joo J. Active flow control using high-frequency compliant structures. Journal of Aircraft. 2004;41(3):603–609.

170. McManus K, Legner H, Davis S. Pulsed vortex generator jets for active flow control. Wright–Patterson AFB (OH): Air Force Research Laboratory (US); 1997. Report No.: AFRL-VA-WP-TR-1998-3028.

171. Seifert A, Pack LG. Oscillatory control of separation at high Reynolds numbers. AIAA Journal. 1999;37(9):1062–1071.

172. Magill JC, McManus KR. Control of dynamic stall using pulsed vortex generator jets. Proceedings of the 36th AIAA Aerospace Sciences Meeting; 1998.

173. Tilmann CP. Enhancement of transonic airfoil performance using pulsed jets for separation control. ADA413925. 2001 Jan 2001. http://www.dtic.mil /dtic/tr /fulltext/u2/a413925.pdf.

174. STRATASYS. Application brief: polyjet multi-material 3D printing. [accessed 2017 May 30]. http://www.stratasys.com/solutions/additive -manufacturing/multi-material-3d-printing.

175. Olympio KR, Gandhi F. Flexible skins for morphing aircraft using cellular honeycomb cores. Journal of Intelligent Material Systems and Structures. 2009;21(17):1719–1735.

176. Barbarino S, Gandhi F, Webster SD. Design of extendable chord sections for morphing helicopter rotor blades. Proceedings of the ASME Conference on Smart Materials, Adaptive Structures and Intelligent Systems; 2010; Philadelphia, PA.

177. Olympio KR, Gandhi F. Zero Poisson's ratio cellular honeycombs for flex skins undergoing one-dimensional morphing. Journal of Intelligent Material Systems and Structures. 2009;21(17):1737–1753.

178. Alderson A, Alderson KL. Auxetic materials. Proceedings of the Institution of Mechanical Engineers, Part G: Journal of Aerospace Engineering. 2007;221(4):565–575.

179. Bitzer TN. Honeycomb technology: materials, design, manufacturing, applications and testing. Dordrecht (Netherlands): Springer Science & Business Media; 2012.

180. Daynes S, Weaver PM. Design and testing of a deformable wind turbine blade control surface. Smart Materials and Structures. 2012;21(10):1–10.

181. Gong X, Huang J, Scarpa F, Liu Y, Leng J. Zero Poisson's ratio cellular structure for two-dimensional morphing applications. Composite Structures. 2015;134:384–392.

182. Olympio KR, Gandhi F, Asheghian L, Kudva J. Design of a flexible skin for a shear morphing wing. Journal of Intelligent Material Systems and Structures. 2010;21(17):1755–1770.

183. Bubert EA, Woods BKS, Lee K, Kothera CS, Wereley NM. Design and fabrication of a passive 1D morphing aircraft skin. Journal of Intelligent Material Systems and Structures. 2010;21(17):1699–1717.

184. Vocke RD, Kothera CS, Woods BK, Wereley NM. Development and testing of a span-extending morphing wing. Journal of Intelligent Material Systems and Structures. 2011;22(9):879–890.

185. Moser P, Barbarino S, Gandhi F. Helicopter rotor-blade chord extension morphing using a centrifugally actuated von Mises truss. Journal of Aircraft. 2014;51(5):1422–1431.

186. Liu W, Zhu H, Zhou S Z, Bai Y, Wang Y, Zhao C. In-plane corrugated cosine honeycomb for 1D morphing skin and its application on variable camber wing. Chinese Journal of Aeronautics. 2013;26(4):935–942.

187. Runkel F, Molinari G, Arrieta AF, Ermanni P. Shape adaptation of wing structures by chiral structures undergoing elastic instability. Proceedings of the 25th AIAA/AHS Adaptive Structures Conference; 2017 Jan 9–13; Grapevine, TX.

188. Martin J, Heyder-Bruckner J-J, Remillat C, Scarpa F, Potter K, Ruzzene M. The hexachiral prismatic wingbox concept. Physica Status Solidi B. 2008;245(3):570–577.

189. Hassan MR, Scarpa F, Mohamed NA. In-plane tensile behavior of shape memory alloy honeycombs with positive and negative Poisson's ratio. Journal of Intelligent Material Systems and Structures. 2009;20(8):897–905.

190. Hassan MR, Scarpa F, Ruzzene M, Mohammed NA. Smart shape memory alloy chiral honeycomb. Materials Science and Engineering A. 2008;481:654–657.

191. Okabe Y, Sugiyama H. Shape-variable sandwich structure with SMA honeycomb core and CFRP skins. Proceedings of SPIE. 2009;7288.

192. Luo Q, Tong L. Adaptive pressure-controlled cellular structures for shape morphing I: design and analysis. Smart Materials and Structures. 2013;22(5):055014.

193. Luo Q, Tong L. Adaptive pressure-controlled cellular structures for shape morphing: II. numerical and experimental validation. Smart Materials and Structures. 2013;22(5):055015.

194. Sun J, Gao H, Scarpa F, Lira C, Liu Y, Leng J. Active inflatable auxetic honeycomb structural concept for morphing wingtips. Smart Materials and Structures. 2014;23(12):125023–125033.

195. Vos R, Barrett R. Mechanics of pressure-adaptive honeycomb and its application to wing morphing. Smart Materials and Structures. 2011;20(9):094010.

196. Vos R. Mechanics and applications of pressure adaptive honeycomb [dissertation]. [Lawrence (KS)]: University of Kansas; 2009.

197. Vos R, Barrett R, Romkes A. Mechanics of pressure-adaptive honeycomb. Journal of Intelligent Material Systems and Structures. 2011;22(10):1041–1055.

198. Vasista S, Tong L. Design and testing of pressurized cellular planar morphing structures. AIAA Journal. 2012;50(6):1328–1338.

199. Rafsanjani A, Akbarzadeh A, Pasini D. Snapping mechanical metamaterials under tension. Advanced Materials. 2015;27(39):5931–5935.

200. Prasad J, Diaz AR. Synthesis of bistable periodic structures using topology optimization and a genetic algorithm. Journal of Mechanical Design. 2006;128(6):1298–1306.

201. Shan S, Kang SH, Raney JR, Wang P, Fang L, Candido F, Lewis JA, Bertoldi K. Multistable architected materials for trapping elastic strain energy. Advanced Materials. 2015;27(29):4296–4301.

202. Qiu J, Lang JH, Slocum AH. A curved-beam bistable mechanism. Journal of Microelectromechanical Systems. 2004;13(2):137–146.

203. Wang YC, Lakes RS. Extreme stiffness systems due to negative stiffness elements. American Journal of Physics. 2004;72(1):40–50.

204. Nadkarni N, Daraio C, Kochmann DM. Dynamics of periodic mechanical structures containing bistable elastic elements: From elastic to solitary wave propagation. Physical Review E. 2014;90(2):023204.

205. Grima JN, Evans KE. Auxetic behavior from rotating squares. Journal of Materials Science Letters. 2000;9(17):1563–1565.

206. Rafsanjani A, Pasini D, Team P. Multistable compliant auxetic metamaterials inspired by geometric patterns in islamic arts. Proceedings of APS March Meeting; 2016;61(2).

207. Webb J. Islamic art inspires stretchy, switchable materials. London (UK): BBC News; 2016 Mar 16 [accessed 2016 Mar 16]. http://www.bbc.com/news/science-environment-35818924.

208. Florijn B, Coulais C, van Hecke M. Programmable mechanical metamaterials. Physical Review Letters. 2014;113(17):175503.

209. Correa DM, Klatt T, Cortes S, Haberman M, Kovar D, Seepersad C. Negative stiffness honeycombs for recoverable shock isolation. Rapid Prototyping Journal. 2015;21(2):193–200.

210. Hu N, Burgueño R. Buckling-induced smart applications: recent advances and trends. Smart Materials and Structures. 2015;24(6):063001.

211. Diaconu CG, Weaver PM, Mattioni F. Concepts for morphing airfoil sections using bi-stable laminated composite structures. Thin-Walled Structures. 2008;46(6):689–701.

212. Daynes S, Weaver PM, Potter KD. Aeroelastic study of bistable composite airfoils. Journal of Aircraft. 2009;46(6):2169–2174.

213. Daynes S, Nall SJ, Weaver PM, Potter k, Margaris P, Mellor PH. Bistable composite flap for an airfoil. Journal of Aircraft. 2010;47(1):334–338.

214. Eckstein E, Pirrera A, Weaver P.M. Multi-mode morphing using initially curved composite plates. Composite Structures. 2014;109:240–245.

215. Daynes S, Potter KD, Weaver PM. Bistable prestressed buckled laminates. Composites Science and Technology. 2008;68(15):3431–3437.

216. Mattioni F, Weaver PM, Friswell MI, Potter KD. Modelling and applications of thermally induced multistable composites with piecewise variation of lay-up in the planform. Proceedings of the 48th AIAA/ASME/ASCE/AHS/ASC Structures, Structural Dynamics and Materials Conference; 2007; Honolulu, HI.

217. Lachenal X, Daynes S, Weaver PM. A non-linear stiffness composite twisting i-beam. Journal of Intelligent Material Systems and Structures. 2013;25(6):744–754.

218. Lachenal X, Weaver PM, Daynes S. Multi-stable composite twisting structure for morphing applications. Proceedings of the Royal Society A; 2012 Jan. doi: 10.1098/rspa.2011.0631.

219. Ai Q, Weaver P. A novel span-wise morphing trailing edge concept. Proceedings of the 25th AIAA/AHS Adaptive Structures Conference; 2017 Jan 9–13; Grapevine, TX.

220. Lachenal X, Daynes S, Weaver PM. A zero torsional stiffness twist morphing blade as a wind turbine load alleviation device. Smart Materials and Structures. 2013;22(6):65016–65028.

221. Mattioni F, Gatto A, Weaver, Friswell, MI, Potter KD. The application of residual stress tailoring of snap-through composites for variable sweep wings. Proceedings of the 47th AIAA/ASME/ASCE/AHS/ASC Structures, Structural Dynamics, and Materials Conference; 2006 May; Newport, RI.

222. Schultz MR. A new concept for active bistable twisting structures. Proceedings of SPIE Smart Structures and Materials. 2005 Mar;5764:241–252.

223. Schultz MR. A concept for airfoil-like active bistable twisting structures. Journal of Intelligent Material Systems and Structures. 2007;19(2):157–169.

224. Portela P, Camanho P, Weaver P, Bond I. Analysis of morphing, multi-stable structures actuated by piezoelectric patches. Computers & Structures. 2008;86(3):347–356.

225. Hufenbach W, Gude M, Kroll L. Design of multistable composites for application in adaptive structures. Composites Science and Technology. 2002;62(16):2201–2207.

226. Hufenbach W, Gude M, Czulak A. Actor-initiated snap-through of unsymmetric composites with multiple deformation states. Journal of Materials Processing Technology. 2006;175(1):225–230.

227. Arrieta AF, Bilgen O, Friswell MI, Hagedorn P. Dynamic control for morphing of bi-stable composites. Journal of Intelligent Material Systems and Structures. 2013;24(3):266–273.

228. Bilgen O, Arrieta AF, Friswell MI, Hagedorn P. Dynamic control of a bistable wing under aerodynamic loading. Smart Materials and Structures. 2013;22(2):25020–25034.

229. Iqbal K, Pellegrino S. Bi-stable composite shells. Proceedings of the 41st AIAA/ASME/ASCE/AHS/ASC Structures, Structural Dynamics, and Materials Conference; 2000; Atlanta, GA.

230. Murphey TW, Pellegrino S. A novel actuated composite tape-spring for deployable structures. Proceedings of the 45th AIAA/ASME/ASCE/AHS

/ASC Structures, Structural Dynamics, and Materials Conference; 2004; Reston, VA.

231. Norman AD, Seffen KA, Guest SD. Multistable corrugated shells. Proceedings of the Royal Society A: Mathematical, Physical and Engineering Science. 2008;464(2095):1653–1672.

232. Dai F, Li H, Du S. A multi-stable lattice structure and its snap-through behavior among multiple states. Composite Structures. 2013;97:56–63.

233. Potter KD, Weaver PM. A concept for the generation of out-of-plane distortion from tailored FRP laminates. Composites Part A: Applied Science and Manufacturing. 2004;35(12):1353–1361.

234. Li H, Dai F, Weaver PM, Du S. Bistable hybrid symmetric laminates. Composite Structures. 2014;116:782–792.

235. McDaniel T, inventor. No assignee. Flying machine. United States patent US 1,905,298. 1933 Apr 25.

236. Norris RK, Pulliam WJ. Historical perspective on inflatable wing structures. Proceedings of the 50th AIAA/ASME/ASCE/AHS/ASC Structures, Structural Dynamics, and Materials Conference; 2009; Palm Springs, CA.

237. Smith TR, McCoy E, Krasinski M, Limaye S, Shook L, Uhelsky F, Graham W. Ballute and parachute decelerators for FASM/Quicklook UAV. Proceedings of the 17th AIAA Aerodynamic Decelerator Systems Technology Conference and Seminar; 2003; Monterey, CA.

238. Cadogan D, Graham W, Smith T. Inflatable and rigidizable wing for unmanned aerial vehicles. Proceedings of the 2nd AIAA Unmanned Unlimited Conference, Workshop, and Exhibit; 2003; San Diego, CA.

239. Cadogan D, Scarborough S, Gleeson D, Dixit A. Recent development and test of inflatable wings. Proceedings of the 47th AIAA/ASME/ASCE/AHS/ASC Structures, Structural Dynamics, and Materials Conference; 2006; Newport, RI.

240. Rendall TCS, Chang C, Marzocca P, Bollt E, Zamankhan P. Aeroelastic Behaviour of a non-rigidizable inflatable UAV wing. Proceedings of the 47th AIAA/ASME/ASCE/AHS/ASC Structures, Structural Dynamics, and Materials Conference; 2006 May; Newport, RI.

241. Murray JE, Pahle JW, Thornton SV, Vogus S, Frackowiak T, Mello J, Norton B. Ground and flight evaulation of a small-scale inflatable-winged aircraft. Edwards AFB (CA): NASA, Dryden Right Research Center; 2002.

242. Simpson AD, Rawashdeh OA, Smith SW, Jacob JDE, Smith WT, Lumpp JE. BIG BLUE: high-altitude UAV demonstrator of Mars airplane technology. Proceedings of the IEEE Aerospace Conference. 2005 Mar; Big Sky, MT.

243. Smith SW, Jacob JD, Jone R, Scarborough S, Cadogan D. A high-altitude test of inflatable wings for low-density flight applications. Proceedings of the 7th AIAA Gossamer Spacecraft Forum; 2006 May; Newport, RI.

244. Simpson A, Usui M, Jacob J, Smith S. Aeromechanics of inflatable airfoils. Proceedings of the 34th AIAA Fluid Dynamics Conference and Exhibit; 2004; Portland, OR.

245. Simpson AD, Usui M, Smith SW, Jacob JD. Development and flight testing of a UAV with inflatable-rigidizable wings. Proceedings of the 42nd AIAA Aerospace Sciences Meeting and Exhibit; 2004; Reno, NV.

246. Simpson A, Jacob J, Smith S. Flight control of a UAV with inflatable wings with wing warping. Proceedings of the 24th Applied Aerodynamics Conference; 2006; San Francisco, CA.

247. Jacob J, Simpson A, Smith S. Design and flight testing of inflatable wings with wing warping. Proceedings of the SAE World Aerospace Congress; 2005; Dallas, TX.

248. Simpson A, Jacob J, Smith S, Rawahdeh O, Lumpp J, Smith W. BIG BLUE II: Mars aircraft prototype with inflatable-rigidizable wings. Proceedings of the 43rd AIAA Aerospace Sciences Meeting and Exhibit; 2005; Reno, NV.

249. Haight AEH, Allred RE, Harrah, LA, McElroy PM, Scarborough SE, Smith T. Design and fabrication of light rigidizable inflatable wings. Proceedings of the 47th AIAA/ASME/ASCE/AHS/ASC Structures, Structural Dynamics, and Materials Conference; 2006 May; Newport, RI.

250. Simpson AS, Smith W, Jacob J. Aeroelastic behavior of inflatable wings: wind tunnel and flight testing. Proceedings of the 45th AIAA Aerospace Sciences Meeting and Exhibit; 2007 Jan; Reno, NV.

251. Murray G, Gandhi F, Bakis C. Flexible matrix composite skins for one-dimensional wing morphing. Journal of Intelligent Material Systems and Structures. 2010;21(17):1771–1781.

252. Bubert EA. Highly extensible skin for a variable wing-span morphing aircraft utilizing pneumatic artificial muscle actuation [thesis]. [College Park (MD)]: University of Maryland; 2009.

253. Woods BK, Kothera CS, Wereley NM. Wind tunnel testing of a helicopter rotor trailing edge flap actuated via pneumatic artificial muscles. Journal of Intelligent Material Systems and Structures. 2011;22(13):1513–1528.

254. Pierce RC, inventor. No assignee. Expansible cover. United States patent US 2,041,950. 1936 May 26.

255. De Haven H, inventor. No assignee. Tensioning device for producing a linear pull. United States patent US 2,483,088. 1949 Sept 27.

256. Takagi T, Sakaguchi Y, inventors. Bridgestone Corporation, assignee. Pneumatic actuator for manipulator. United States patent US 4,615,260. 1986 Oct 7.

257. Inoue K. Rubbertuators and applications for robots. Proceedings of the 4th International Symposium on Robotics Research; 1988; Santa Cruz, CA.

258. Zhang Z, Philen M. Review: pressurized artificial muscles. Journal of Intelligent Material Systems and Structures. 2012;23(3):255–268.

259. Shadow Robot Company [accessed 2016 Jan 5]. http://www .shadowrobot.com.

260. Festo. Fluidic muscle DMSP/MAS. Esslingen am Neckar (Germany): Festo; 2013.

261. Festo, DMSP/MAS product flyer. Esslingen am Neckar (Germany): Festo; 2015.

262. Verrelst B, Van Ham R, Vanderborght B, Lefeber D, Daerden F, Van Damme, M. Second generation pleated pneumatic artificial muscle and its robotic applications. Advanced Robotics. 2006;20(7):783–805.

263. Verrelst B, Van Ham R, Vanderborght B, Daerden F, Lefeber D, Vermuelen J. The pneumatic biped “Lucy” actuated with pleated pneumatic artificial muscles. Autonomous Robots. 2005;18(2):201–213.

264. Villegas D, Van Damme M, Vanderborght B, Beyl P, Lefeber D. Third-generation pleated pneumatic artificial muscles for robotic applications: development and comparison with McKibben muscle. Advanced robotics. 2012;26(11–12):1205–1227.

265. Van Damme M, Daerden F, Lefeber D. A pneumatic manipulator used in direct contact with an operator. Proceedings of the IEEE International Conference on Robotics and Automation; 2005; Barcelona, Spain.

266. Saga N, Nakamura T, Yaegashi K. Mathematical model of pneumatic artificial muscle reinforced by straight fibers. Journal of Intelligent Material Systems and Structures. 2007;18(2):175–180.

267. Nakamura T, Shinohara H. Position and force control based on mathematical models of pneumatic artificial muscles reinforced by straight glass fibers. Proceedings of the IEEE International Conference on Robotics and Automation; 2007; Rome, Italy.

268. Bertetto AM, Ruggiu M. Characterization and modeling of air muscles. Mechanics Research Communications. 2004;31(2):185–194.

269. Saga N, Saikawa T, Okano H. Flexor mechanism of robot arm using pneumatic muscle actuators. Proceedings of the IEEE International Conference on Mechatronics and Automation; 2005; Niagara Falls, Canada.

270. Peel LD, Mejia J, Narvaez B, Thompson Kyle, Lingala M. Development of a simple morphing wing using elastomeric composites as skins and actuators. Journal of Mechanical Design. 2009;131(9):091003.

271. Wereley NM, Kothera C, Bubert E, Woods B, Gentry M, Vocke R. Pneumatic artificial muscles for aerospace applications. Proceedings of the 50th AIAA/ASME/ASCE/AHS/ASC Structures, Structural Dynamics, and Materials Conference; 2009 May; Palm Springs, CA.

272. Woods BK, Kothera CS, Sirohi J, Wereley NM. Pneumatic artificial muscles for trailing edge flap actuation: a feasibility study. Smart Materials and Structures. 2011;20(10):105021.

273. Chou CP, Hannaford B. Measurement and modeling of McKibben pneumatic artificial muscles. IEEE Transactions on Robotics and Automation. 1996;12(1):90–102.

274. Davis S, Tsagarakis N, Canderle J, Darwin JC. Enhanced modelling and performance in braided pneumatic muscle actuators. The International Journal of Robotics Research. 2003;22(3–4):213–227.

275. Chen Y, Yin W, Liu Y, Leng J. Structural design and analysis of morphing skin embedded with pneumatic muscle fibers. Smart Materials and Structures. 2011;20(8):085033.

276. Shan Y, Bakis CE. Flexible matrix composite actuators. Proceedings of the 20th Annual Technical Conference of American Society for Composites; 2005; Philadelphia, PA.

277. Thill C, Etches J, Bond I, Potter K. Morphing skins. The Aeronautical Journal. 2008;112(1129):117–139.

278. Feng N, Liu L, Liu Y, Leng J. A bio-inspired, active morphing skin for camber morphing structures. Smart Materials and Structures. 2015;24(3):035023.

279. Peel LD, Baur JW, Justice RS. Characterization and application of shape-changing panels with embedded rubber muscle actuators. Smart Materials and Structures. 2013;22(9):094020.

280. Felt W, Remy CD. Smart braid: air muscles that measure force and displacement. Proceedings of the IEEE/RSJ International Conference on Intelligent Robots and Systems; 2014; Chicago, IL.

281. Park YL, Wood RJ. Smart pneumatic artificial muscle actuator with embedded microfluidic sensing. IEEE Sensors; 2013;13(1).

282. Jung K, Kim KJ, Choi HR. A self-sensing dielectric elastomer actuator. Sensors and Actuators A: Physical. 2008;143(2):343–351.

283. Goulbourne NC, Son S, Fox JW. Self-sensing McKibben actuators using dielectric elastomer sensors. Proceedings of the 14th International Symposium on Smart Structures and Materials and Nondestructive Evaluation and Health Monitoring; 2007; San Diego, CA.

284. Shan Y, Lotfi A, Philen M, Wang K-W. Fluidic flexible matrix composites for autonomous structural tailoring. Proceedings of SPIE. 2007 Mar; 6525.

285. Youn EB, Silton SI. Numerical study on bending body projectile aerodynamics. Proceedings of the 34th AIAA Applied Aerodynamics Conference; 2016 June 13–17; Washington, DC.

286. Paul JL. Aerodynamic optimization of a supersonic bending body projectile by a vector-evaluated genetic algorithm. Aberdeen Proving Ground (MD): Army Research Laboratory (US); 2016 Dec. Report No.: ARL-CR-0810.

287. Kota S. Shape-shifting things to come. Scientific American. 2014;310(5):58–65.

288. Park YL, Santos J, Galloway KG, Goldfield EC, Wood RJ. A soft wearable robotic device for active knee motions using flat pneumatic artificial muscles. Proceedings of the IEEE International Conference on Robotics & Automation (ICRA); 2014 May 31–June 7; Hong Kong.

289. Bishop-Moser J, Krishnan G, Kota S. Force and moment generation of fiber-reinforced pneumatic soft actuators. Proceedings of the IEEE/RSJ International Conference on Intelligent Robots and Systems; 2013; Tokyo, Japan.

290. Bishop-Moser J, Krishnan G, Kim C, Kota S. Design of soft robotic actuators using fluid-filled fiber-reinforced elastomeric enclosures in parallel combinations. Proceedings of the IEEE/RSJ International Conference on Intelligent Robots and Systems; 2012; Vilamoura-Algarve, Portugal.

291. Bishop-Moser JL. Design of generalized fiber-reinforced elasto-fluidic systems [dissertation]. [Ann Arbor (MI)]: University of Michigan; 2014.

292. Philen MK, Shan Y, Prakash P, Wang KW, Rahn CD, Zydney AL, Bakis CE. Fibrillar network adaptive structure with ion-transport actuation. Journal of Intelligent Material Systems and Structures. 2007;18(4):323–334.

293. Faudzi AAM, Razif MRM, Aimi IN, Hirooka D. Development of bending soft actuator with different braided angles. Proceedings of the IEEE/ASME International Conference on Advanced Intelligent Mechatronics (AIM); 2012; Kaohsiung, Taiwan.

294. Galloway KC, Polygerionos P, Walsh CJ, Wood RJ. Mechanically programmable bend radius for fiber-reinforced soft actuators. Proceedings of the 16th International Conference on Advanced Robotics (ICAR); 2013; Montevideo, Uruguay.

295. Mosadegh B, Polygerionos P, Keplinger C, Wennstedt S, Shepherd RF, Gupta U, Shim J, Bertoldi K, Walsh CJ, Whitesides GM. Pneumatic networks for soft robotics that actuate rapidly. Adv Funct Mater. 2014;24:2163–2170.

296. Polygerinos P, Lyne S, Wang Z, Nicolini LF, Mosadegh B, Whitesides GM, Walsh CJ. Towards a soft pneumatic glove for hand rehabilitation. Proceedings of the IEEE/RSJ International Conference on Intelligent Robots and Systems; 2013; Tokyo, Japan.

297. Peele BN, Wallin TJ, Zhao H, Shepherd RF. 3D printing antagonistic systems of artificial muscle using projection stereolithography. Bioinspiration & Biomimetics. 2015;10(5):055003.

298. Shepherd RF, Stokes AA, Freake J, Barber J, Snyder PW, Mazzeo AD, Cademartiri L, Morin SA, Whitesides GM. Using explosions to power a soft robot. Angewandte Chemie International Edition. 2013;52(10):2892–2896.

299. Bartlett NW, Tolley MT, Overvelde JT, Weaver JC, Mosadegh B, Bertoldi K, Whitesides GM, Wood RJ. A 3D-printed, functionally graded soft robot powered by combustion. Science. 2015;349(6244):161–165.

300. Tolley MT, Shepherd RF, Karpelson M, Bartlett NW, Galloway KC, Wehner M, Nunes Rui, Whitesides GM, Wood RJ. An untethered jumping soft robot. Proceedings of the IEEE/RSJ International Conference on Intelligent Robots and Systems; 2014 Sep; Chicago, IL.

301. Martinez RV, Fish CR, Chen X, Whitesides GM. Elastomeric origami: programmable paper-elastomer composites as pneumatic actuators. Adv Funct Mater. 2012;22:1376–1384.

302. Yao L, Niiyama R, Ou J, Follmer S, Della Silva C, Ishii H. PneUI: pneumatically actuated soft composite materials for shape changing interfaces. Proceedings of the 26th Annual ACM Symposium on User Interface Software and Technology; 2013; St Andrews, UK.

303. Wakimoto S, Suzumori K, Ogura K. Miniature pneumatic curling rubber actuator generating bidirectional motion with one air-supply tube. Advanced Robotics. 2011;25(9–10):1311–1330.

304. Suzumori K, Iikura S, Tanaka H. Development of flexible microactuator and its applications to robotic mechanisms. Proceedings of the IEEE International Conference on Robotics and Automation; 1991; Sacramento, CA.

List of Symbols, Abbreviations, and Acronyms

1-D	1-dimensional
2-D	2-dimensional
AFRL	US Air Force Research Laboratory
AoA	angle of attack
ARL	US Army Research Laboratory
CRAM	counter rocket, artillery, and mortar
DAP	directionally attached piezoelectric
DE	dielectric elastomer
eGaIn	eutectic gallium indium
FASM	Forward Air Support Munition
FMC	flexible matrix composite
L/D	lift to drag
LED	light-emitting diode
MFC	macro-fiber composite
NACA	National Advisory Committee for Aeronautics
NASA	National Aeronautics and Space Administration
PAM	pressurized artificial muscle
PBP	post-buckled precompressed
PPAM	pleated pressurized artificial muscle
PZT	lead zirconate titanate
RAINBOW	Reduced And INternally Biased Oxide Wafer
RF	radio frequency
SMA	shape memory alloy
SMP	shape memory polymer
T_g	glass transition temperature

THUNDER	THin Layer UNimorph Ferroelectric DrivER and Sensor
UV	ultraviolet
ZPR	zero Poisson's ratio

1 (PDF)	DEFENSE TECHNICAL INFORMATION CTR DTIC OCA
2 (PDF)	DIR ARL IMAL HRA RECORDS MGMT RDRL DCL TECH LIB
1 (PDF)	GOVT PRINTG OFC A MALHOTRA
19 (PDF)	ARL RDRL WML E F FRESCONI I CELMINS J BRYSON J DESPIRTO J PAUL J VASILE L FAIRFAX L STROHM P WEINACHT S SILTON RDRL WML F B NELSON T BROWN J CONDAN D EVERSON M HAMAOUI M ILG B KLINE D PETRICK B TOPPER